BIRA·IASB

aeronomie·be

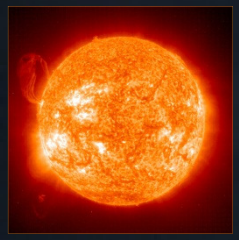

The Dynamics of the Inner Magnetosphere of the Earth

Kris Borremans, Viviane Pierrard, Joseph Lemaire, Juan Cabrera, and the SPENVIS team.

Belgian Institute for Space Aeronomy (IASB-BIRA), Brussels, Belgium

Magnetosphere of the Earth

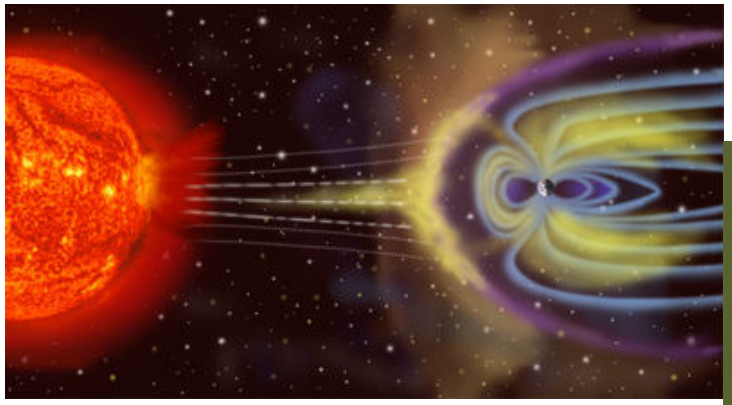

The Dynamics of the magnetosphere is driven by the solar wind

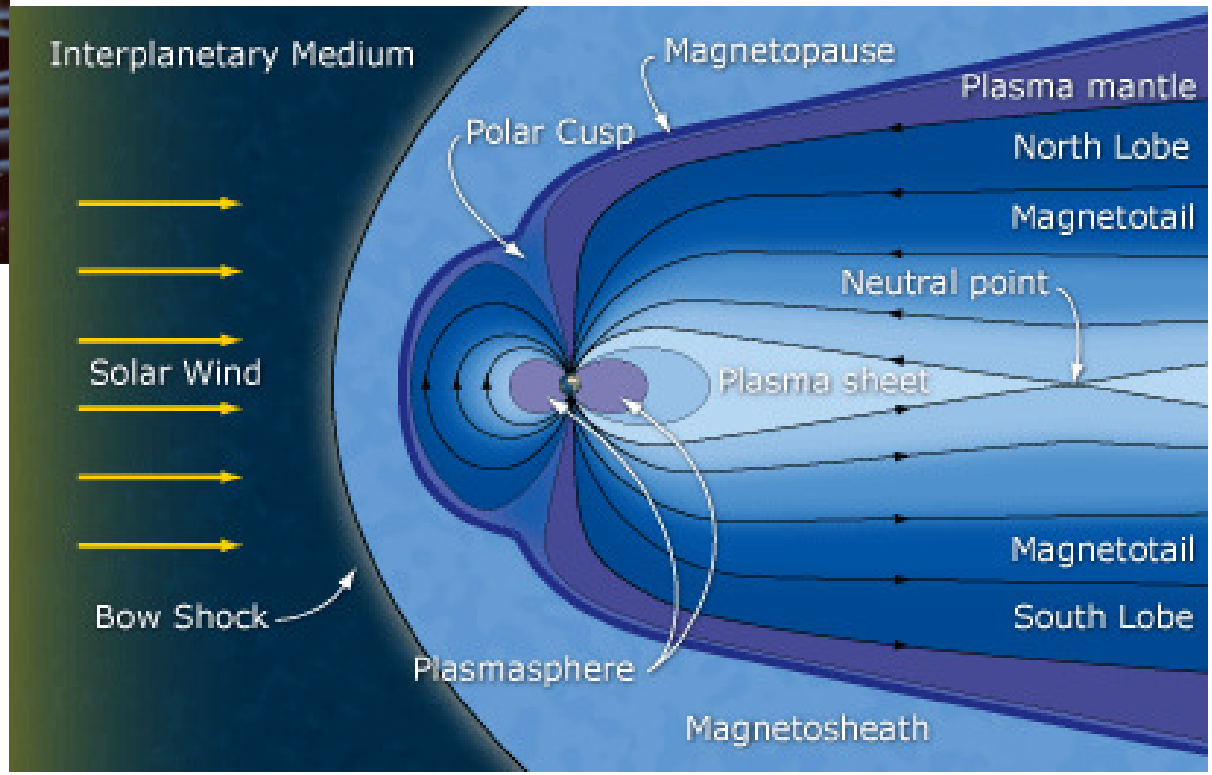

I will discuss the plasmasphere and the radiation belts.

Dynamic magnetic field

Sketch of the Earth's magnetosphere, delimited by the magnetopause (orange dashed line), its border with the solar wind. Reconnection starts at the front of the magnetosphere (left side) and the reconnected field lines (in white) propagate tailward.

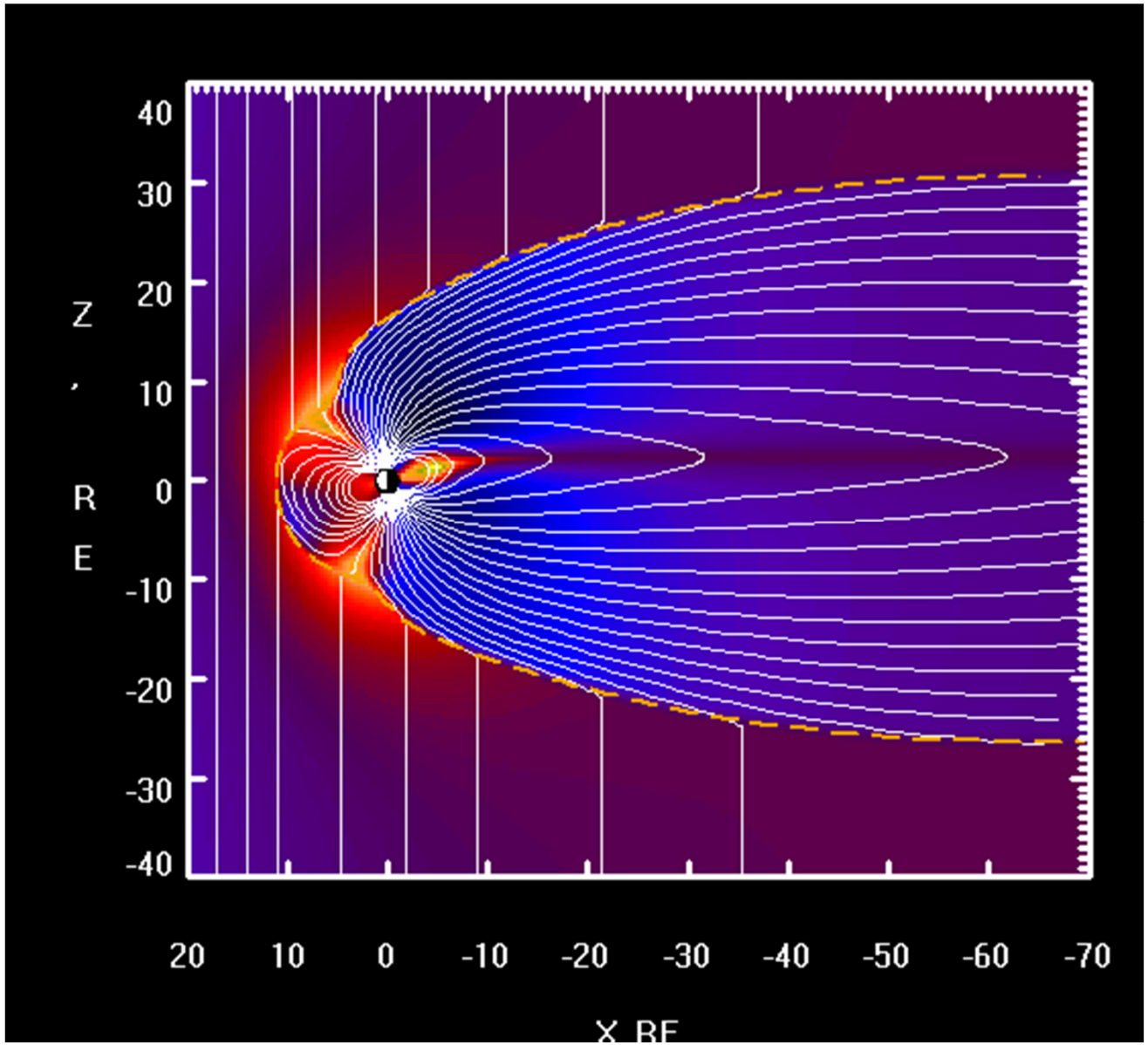

Date: 03 Feb 2005
Satellite: Cluster
Depicts: Reconnecting field lines

http://geo.phys.spbu.ru/~tsyganenko/modeling.html

Plasmasphere: cold particles ~eV

The plasmasphere is the extension of the ionosphere to higher altitudes.
I consists of electrons, protons and ions.

The plasmasphere is important to determine the Total Electron Content.

The ionosphere and the plasmasphere corotate with the Earth.

The dynamics of the plasmasphere is driven by the corotation electric field and the convection electric field.

The plasmasphere can expand to beyond geosynchronous orbit, whereas the plasmapause moves earthward, down to $L < 2\ R_E$ during periods of high geomagnetic activity. (F. Darrouzet, J. De Keyser)

The plasmasphere interacts with the radiation belts via wave-particle interactions.
To model the radiation belts a good plasmasphere model is necessary.

Plasmasphere drift

The motion of the low energy particles is mostly determined by the E cross B drift.

$$\boldsymbol{v}_{\boldsymbol{E}\times\boldsymbol{B}} = \frac{\boldsymbol{E}\times\boldsymbol{B}}{B^2}$$

The E cross B drift is independent of the charge and the mass.
The drift period is approximately 1 day.

For protons and ions the gravitational drift is also important.

$$\boldsymbol{v}_{\boldsymbol{g}} = \frac{m_p}{e}\frac{\boldsymbol{g}\times\boldsymbol{B}}{B^2}$$

The gravitational drift causes polarization.

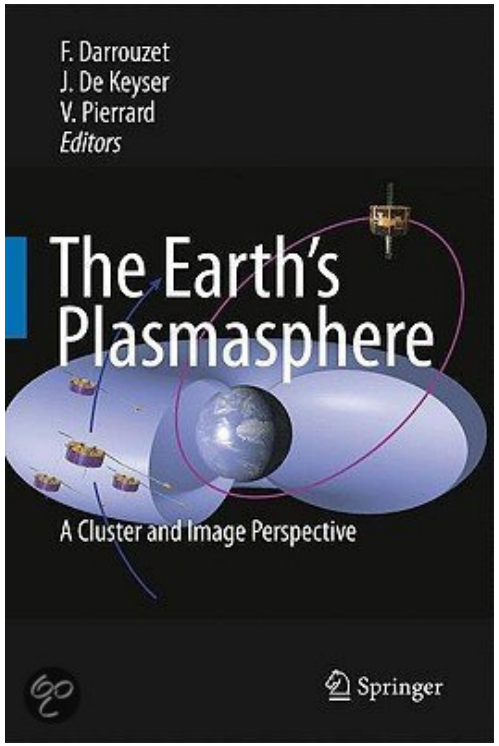

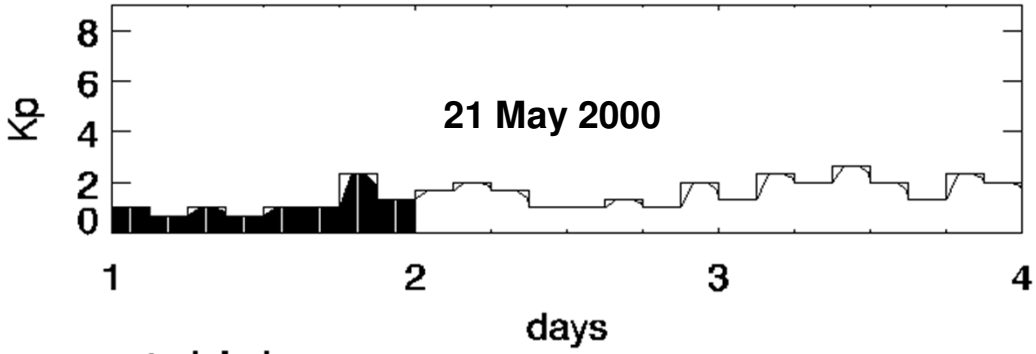

Ionosphere Coupling

The model of the plasmasphere (Pierrard and Stegen, 2008) has been coupled with the ionosphere. We use the empirical International Reference Ionosphere (IRI) from Bilitza and Reinisch (2008) to determine the number density and temperatures of the particles between 60 and 2000 km of altitude. These values are taken as boundary conditions in the plasmasphere model. We coupled the plasmasphere and the ionosphere with logarithmic interpolation (Pierrard and Borremans, 2012a).

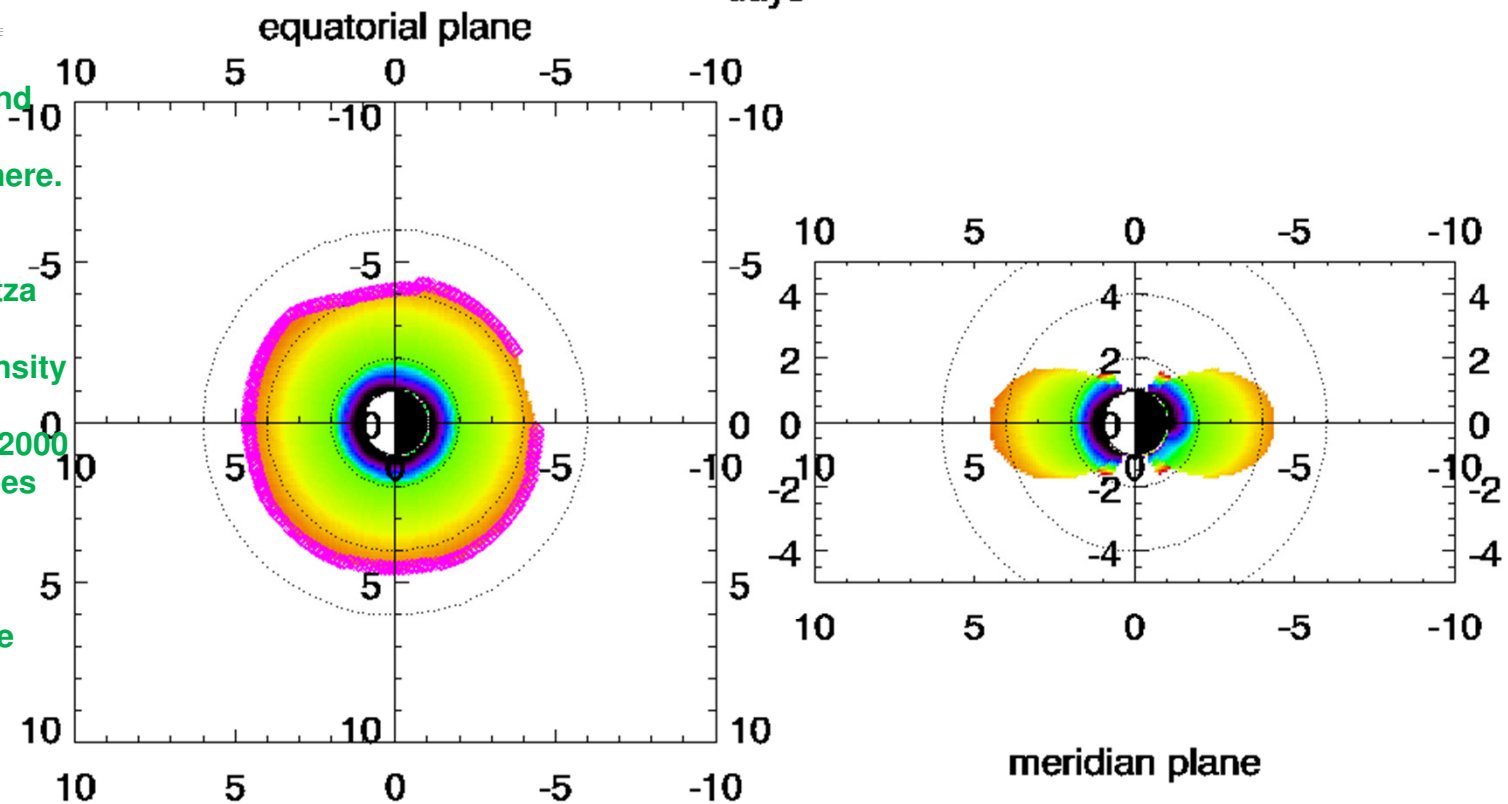

Dynamic Plasmasphere Model

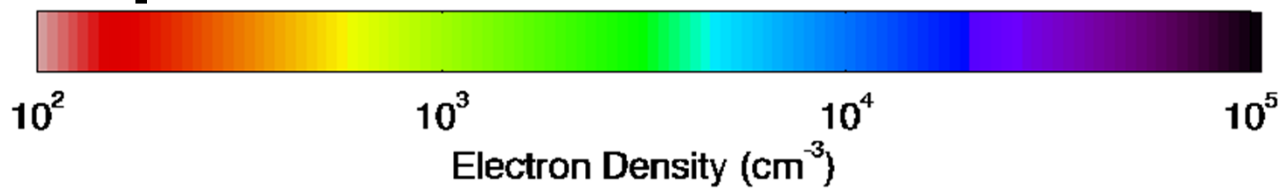

BELGISCH INSTITUUT VOOR RUIMTE-AERONOMIE INSTITUT D'AERONOMIE

Dynamic animations of the plasmasphere

The model is used for nowcasting and **forecasting**. On http://www.spaceweather.eu, the user gives the date of the event as an input. The program retrieves the observed geomagnetic activity level index Kp and calculates the position of the plasmapause and the number density of the electrons predicted by the model. Animated simulations show the dynamical plasmasphere every half hour of the simulated day. The user can also give the corotation velocity fraction between 0.8 and 1.

We developed models for the density and the temperature of the electrons, the protons, and the He ions in the plasmasphere and the plasmatrough.

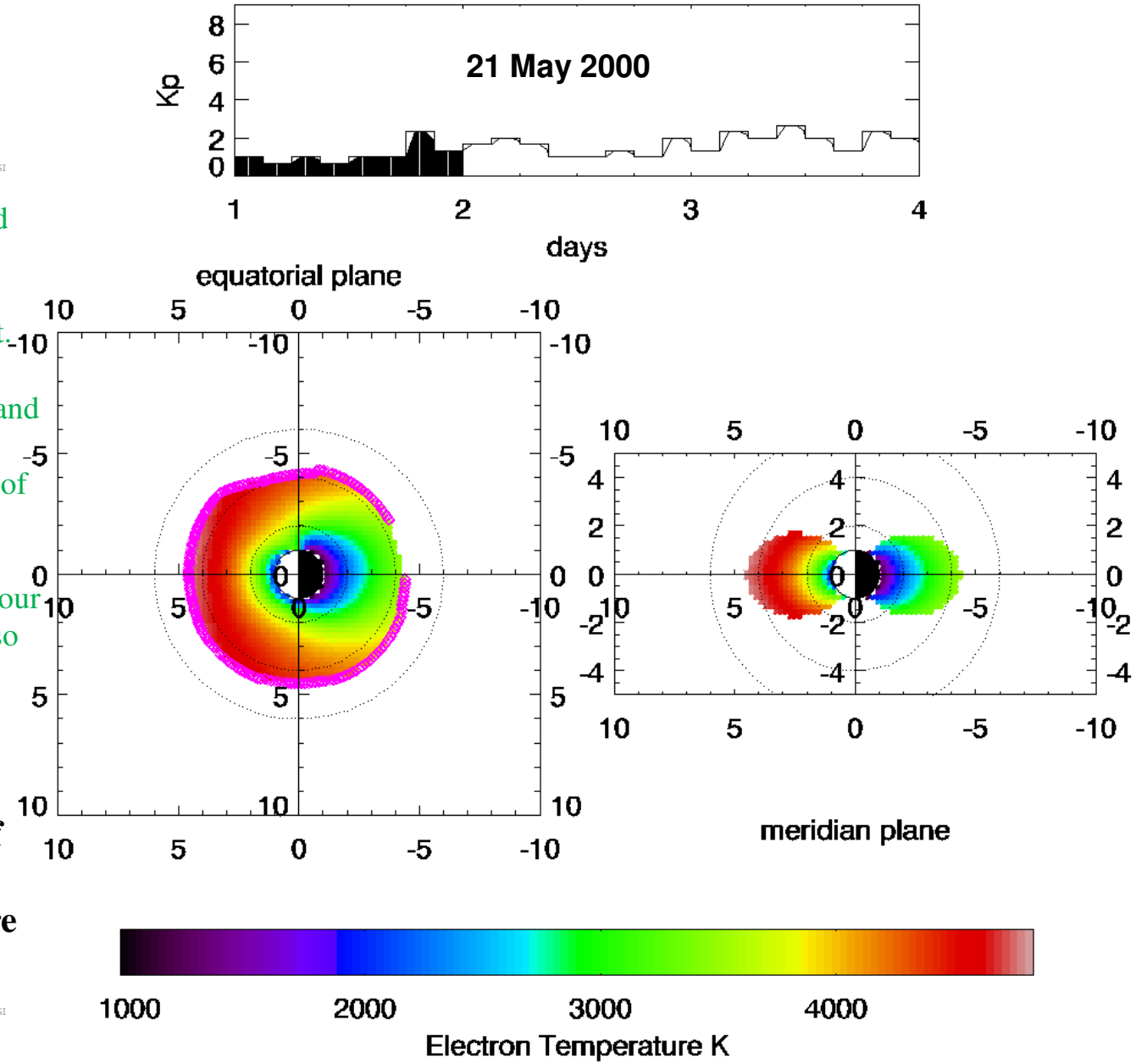

BELGISCH INSTITUUT VOOR RUIMTE-AERONOMIE INSTITUT D'AERONOMIE SPATIALE DE BELGIQUE BELGI

Plasmasphere Model

http://www.spaceweather.eu

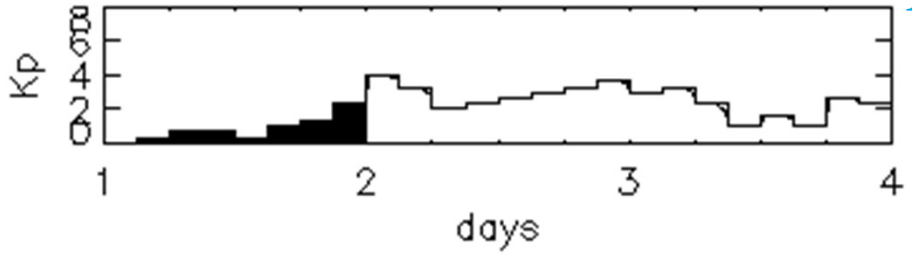

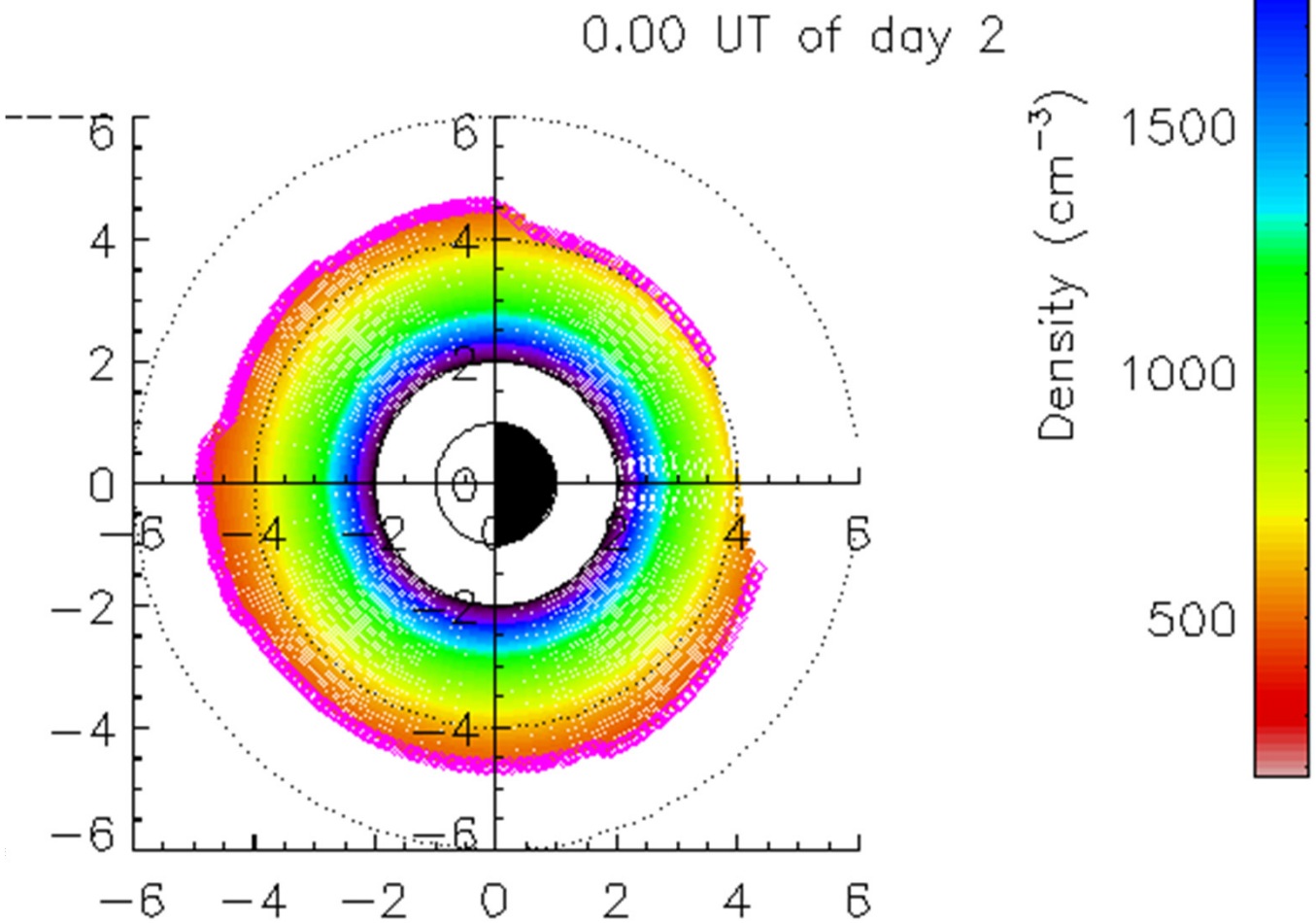

Nowcasting of the plasmasphere

The nowcasting of the plasmasphere is rebuilt every hour and is using the plasmasphere model developed by Pierrard and Stegen (2008). The IRF Kp forecast retrieved from SWENET. In case of missing Kp values linear interpolation is performed.

N INSTITUTE OF SPACE AERONOMY BELGISCH INSTITUUT VOOR RUIMTE-AERONOMIE INSTITUT D'AERO

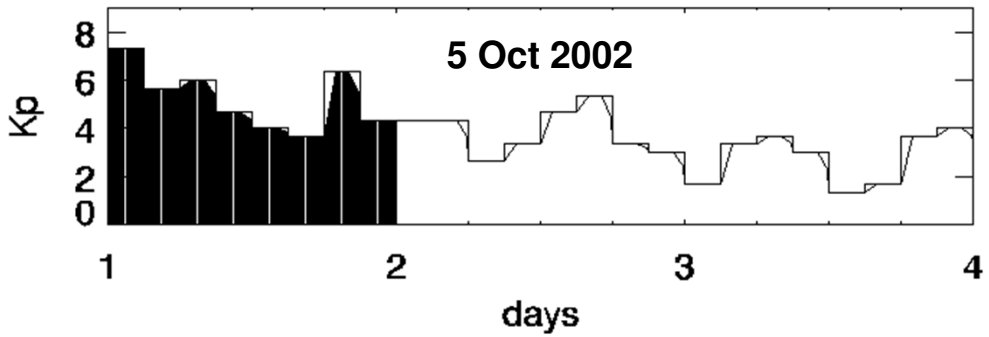

The electron density in the plasmasphere on 5 October 2002 during a geomagnetic storm obtained by the model. In the geomagnetic equatorial plane the plasmapause is given by the purple diamonds, and is illustrating a plume in the afternoon MLT sector in the direction of the Sun.

During a geomagnetic storm the plasmasphere is eroded.
After the geomagnetic storm, the ionosphere refills the plasmasphere.

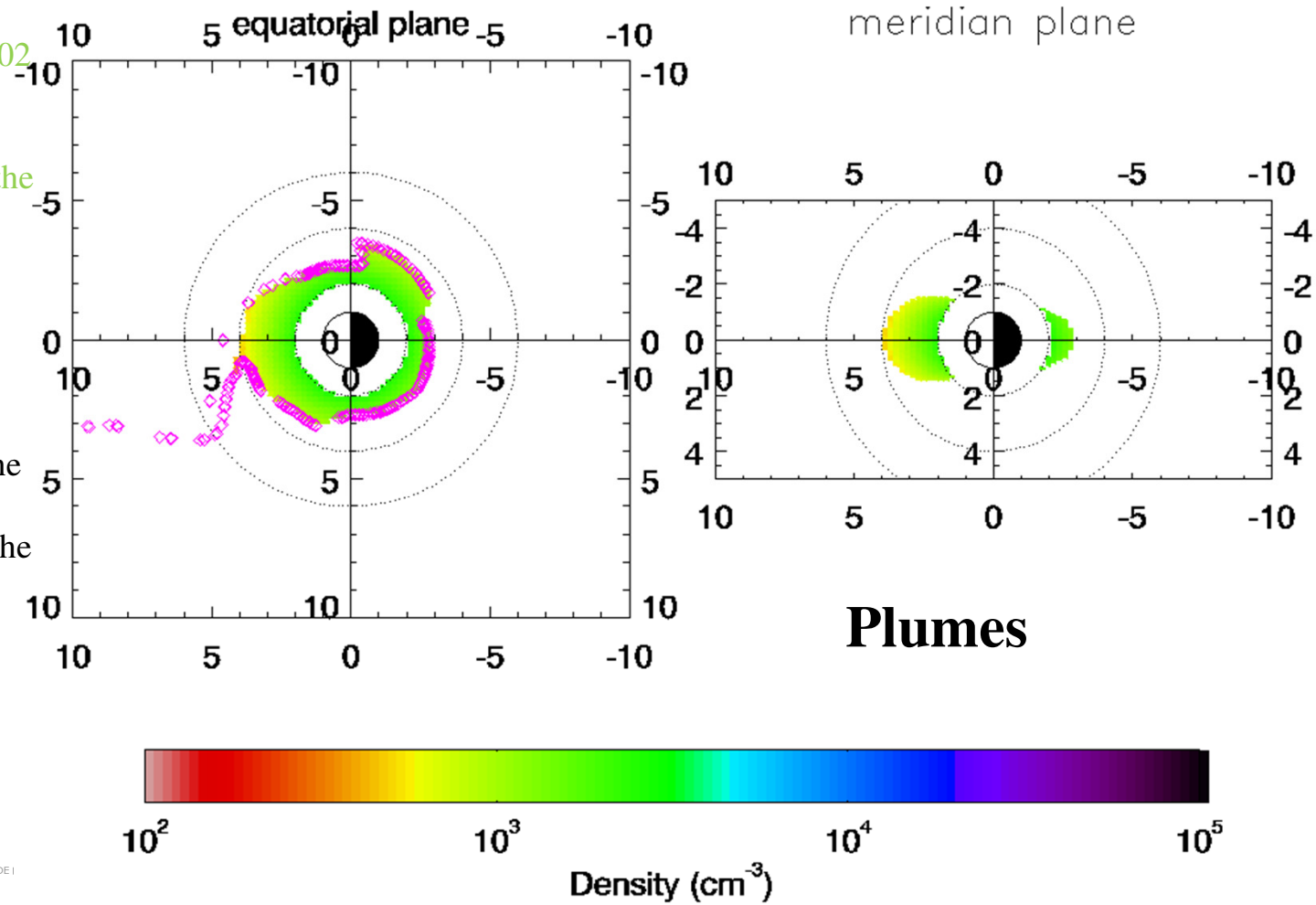

Plumes

The radiation belts are together with the cold plasmaphere quasi-neutral.

In the plasmaphere the particles corotate with the Earth, but in the radiation belts the electrons and the protons drift in opposite directions. This ring current will induce a magnetic field, which can be measured on the surface of the Earth by the Dst index.

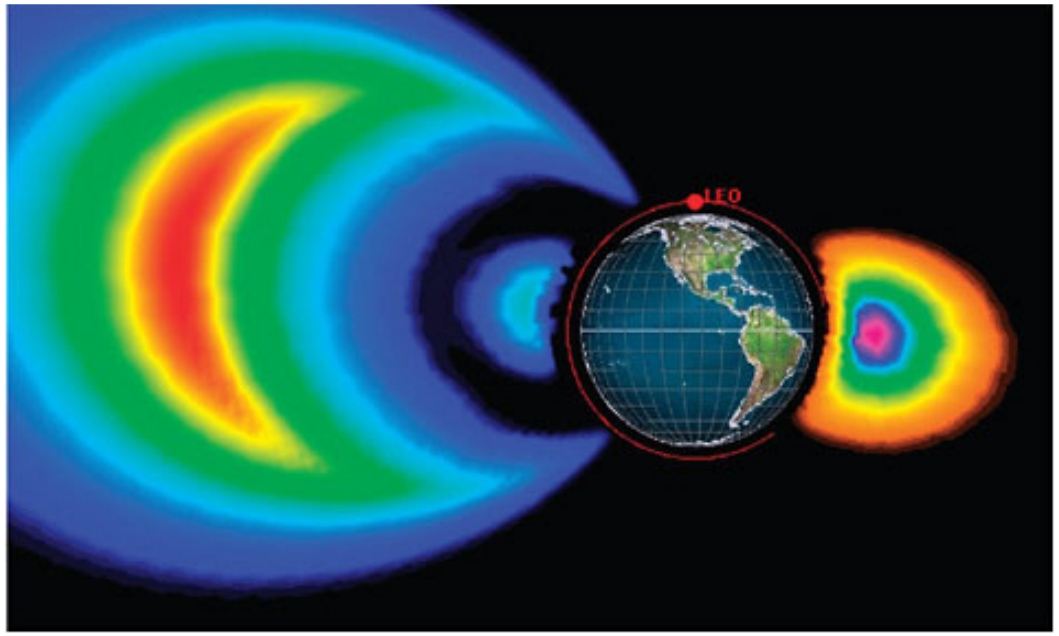

2 Electron Radiation Belts

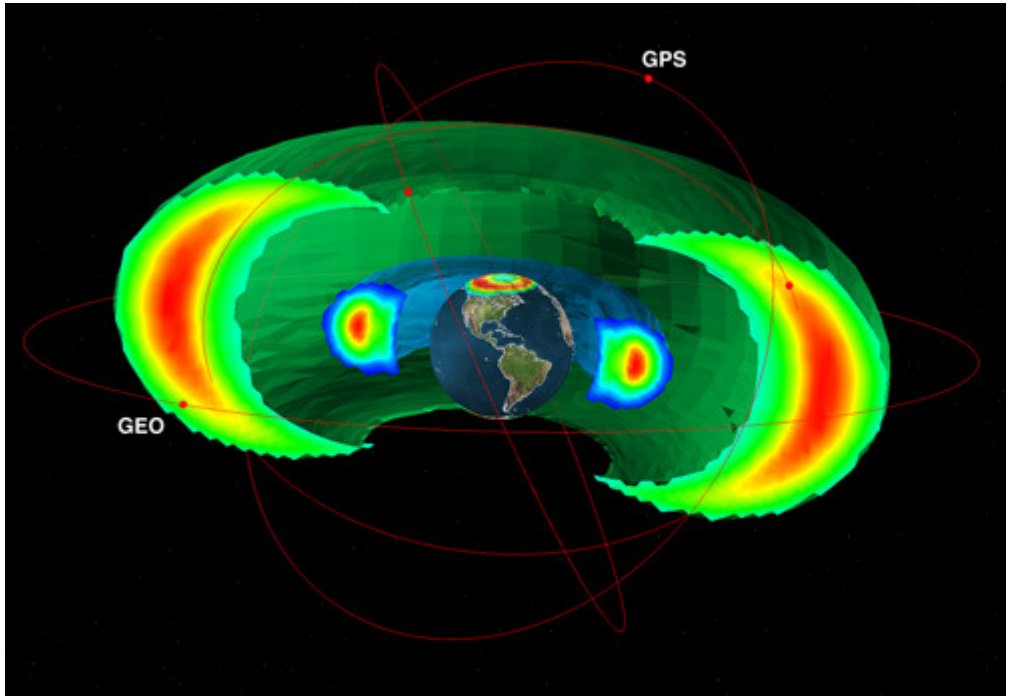

1 Proton Radiation Belt

Radiation belt dynamics is strongly influenced by the core plasmasphere distribution and more specifically, by the position of the plasmapause and by the waves that are able to scatter the energetic particles into their loss cones.

Links between the plasmapause and the radiation belts boundaries from Cluster measurements (F. Darrouzet et al.)

AE8/AP8 is an empirical model for the radiation belts. AE8 gives the electron fluxes in the energy range 0.04 MeV to 7 MeV. AP8 gives the proton fluxes in the energy range 0.1 MeV to 400 MeV. The fluxes are given as a function of the energy of the particle, the L-value, and the B/Bo value. The B/Bo value is the magnetic field strength normalized to its equatorial value on the magnetic field line. The data is from more than 20 satellites from the early sixties to the mid-seventies. AE8-MIN gives the electron fluxes during solar minimum and AE8-MAX gives the electron fluxes during solar maximum.

Static Radiation Belt model AE8

The differential flux is shown for 244 - 406 keV

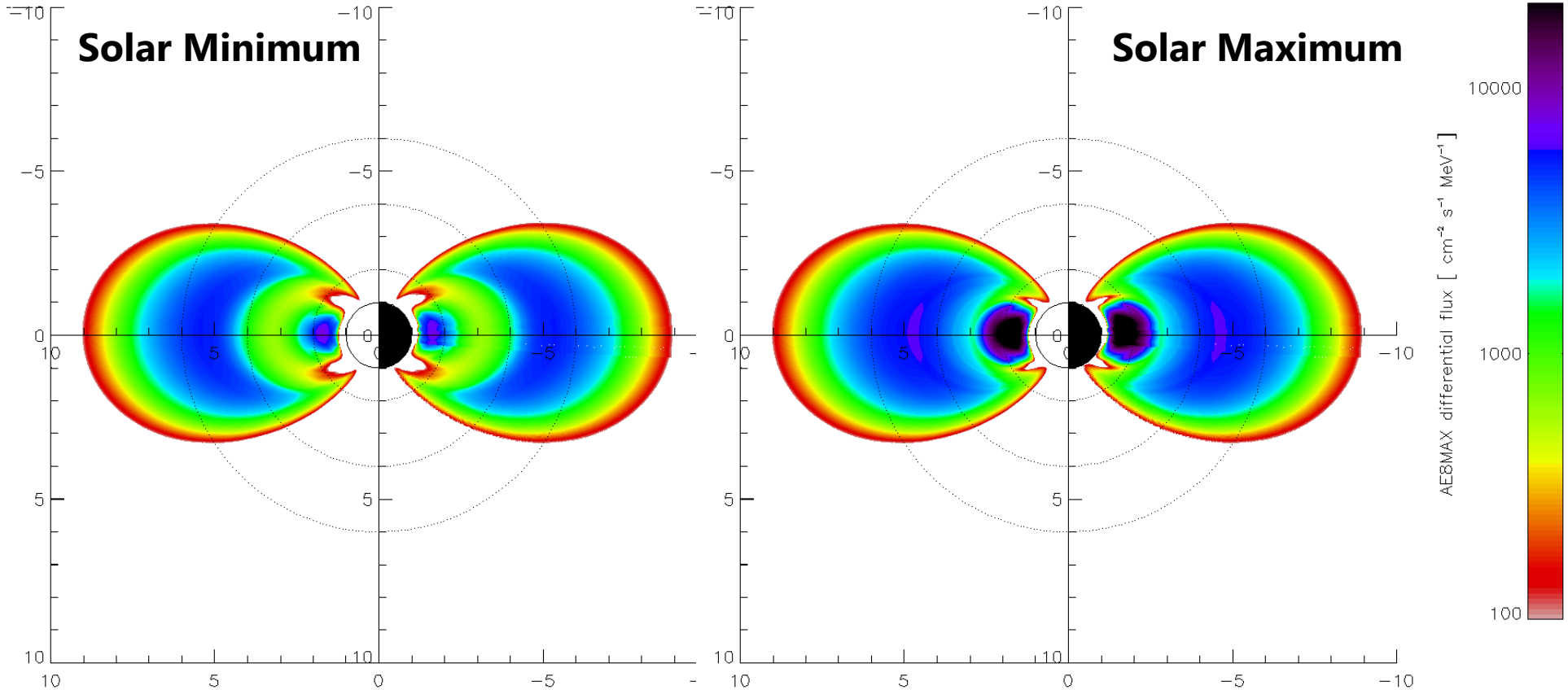

For the outer belt the energy distribution is more or less a Maxwellian distribution.
For electrons it's a sum of 2 Maxwellians. For protons it's a Kappa distribution.
(Pierrard V. and K. Borremans) Fitting the AP8 spectra to determine the proton momentum distribution functions in space radiations

Radiation Belts

Energetic particles: 10 keV - 100 MeV

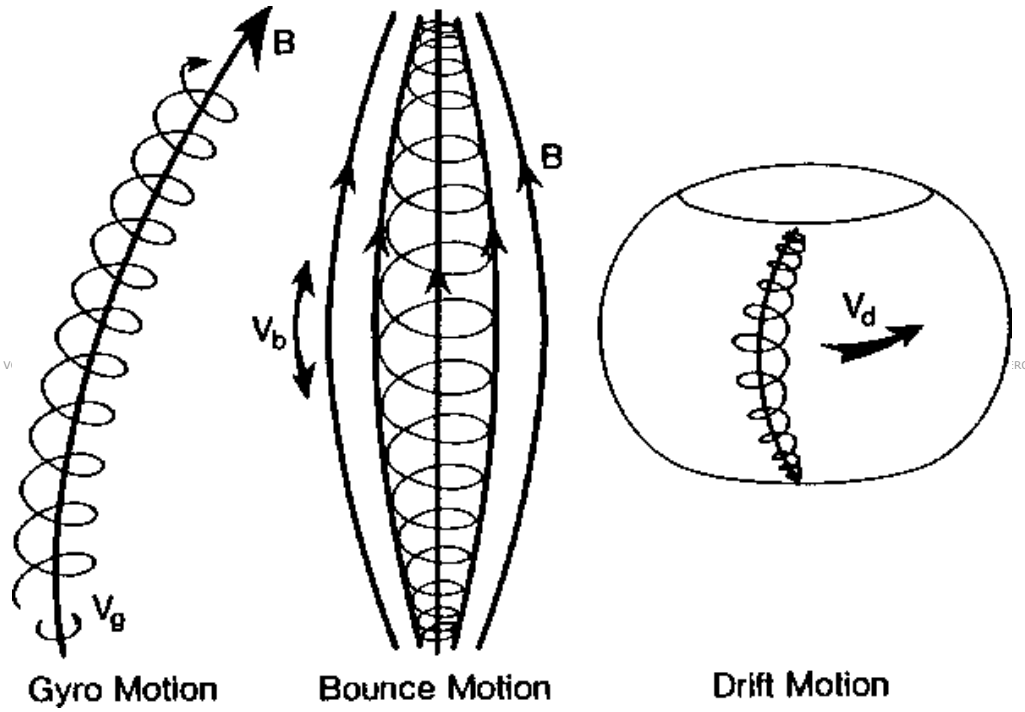

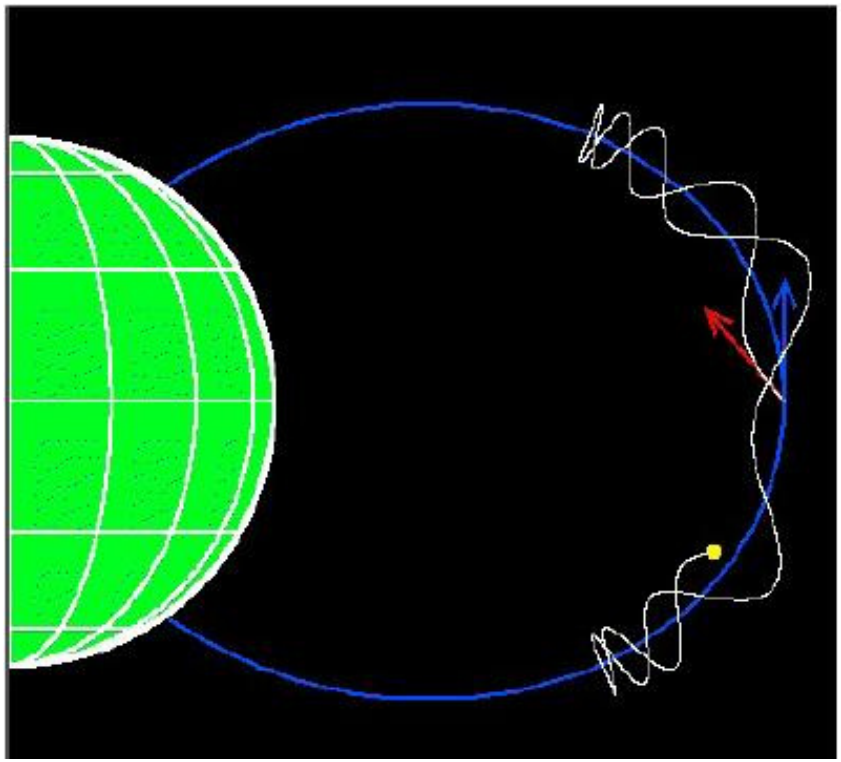

The latitude of the mirror points depend on the pitch angle.

The Cluster mission consists of four identical spacecraft (C1, C2, C3 and C4) launched during the summer of 2000.
The spacecraft fly along polar orbits, with a period of approximately 57h, and an initial perigee of about 4 R_E Since 2007, the perigee of the Cluster orbit has moved closer to the Earth, down to about 1.3 RE in the year 2010. The orbit has also changed from originally being polar to a much lower inclination.
The satellites rotate around their axis 15 times per minute, which is 1 spin every 4 seconds. The RAPID experiment on board Cluster measures energetic particles fluxes.

Cluster Rapid pitch angle distribution

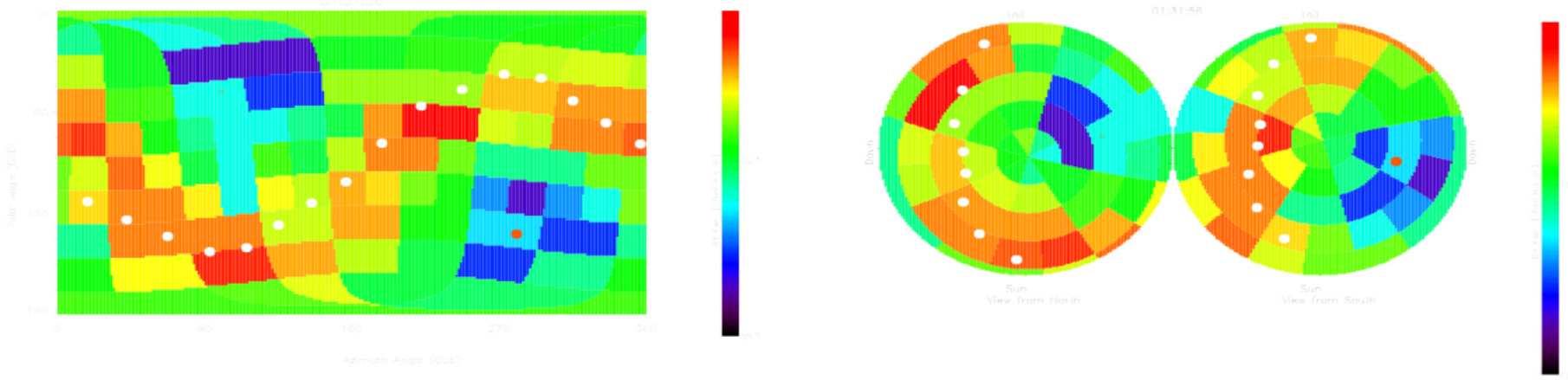

Figure 10: Left: 3-D electron distribution from L3DD data in GSE showing 9 polar directions and 16 azimuthal sectors. Right: The same data but in a bispherical view, whereas the left spheres on both plots show northward flow and the right southward. White dots indicate 90° to the magnetic field, and the red dot and red star mark the calculated direction magnetic field vector.

Most of the particles have a pitch angle of 90 degrees. So they will mirror equatorially.

Electron (> 300 keV) Belt Dynamics (1979-1999)
(from NOAA 5-14 POES Satellites)

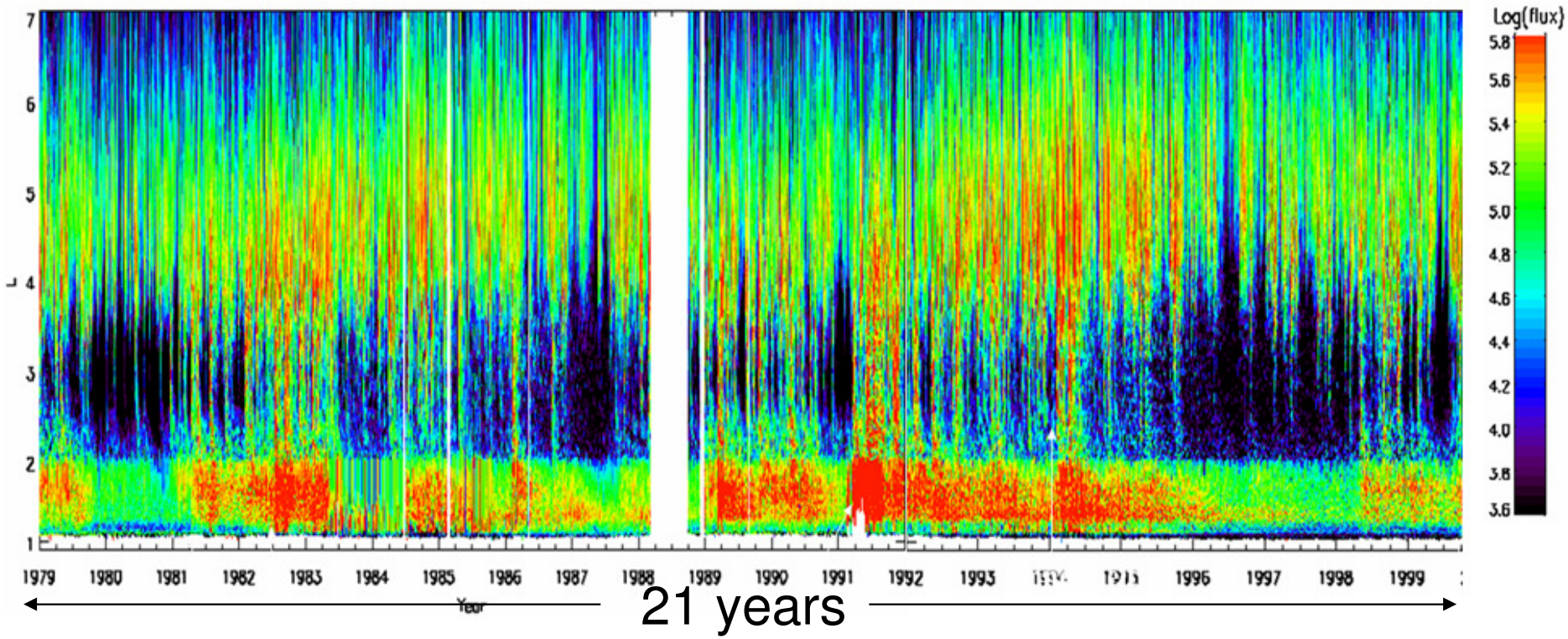

- Inner (peak near L=1.6) and Outer (peak near L= 4-5) Electron Belts; Slot Region (L=3).
- Variability of outer belt; Relative stable inner belt.
- Hazardous to satellites, astronauts, and spacecraft.

Based on CLUSTER satellite measurements, an empirical three dimensional dynamic model of the radiation belts is also in development. This model forecasts the dynamics of the radiation belts based on the predicted Dst (disturbed storm time) index.

Erroneous jumps in the measured fluxes appear due to the auto-switching of the integration time.

Cluster satellites: RAPID instrument

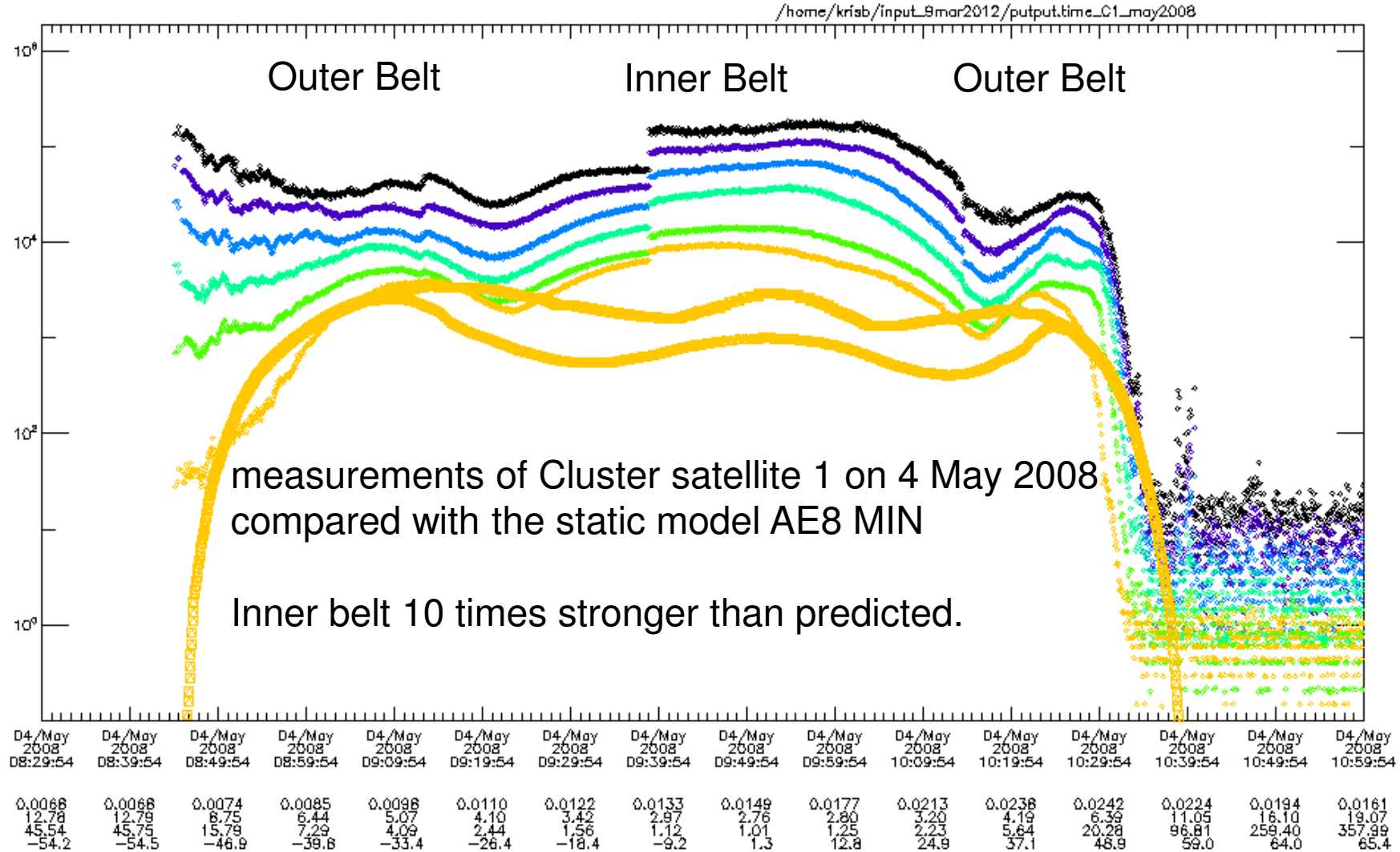

Inner Electron Radiation Belt is stable

L=3

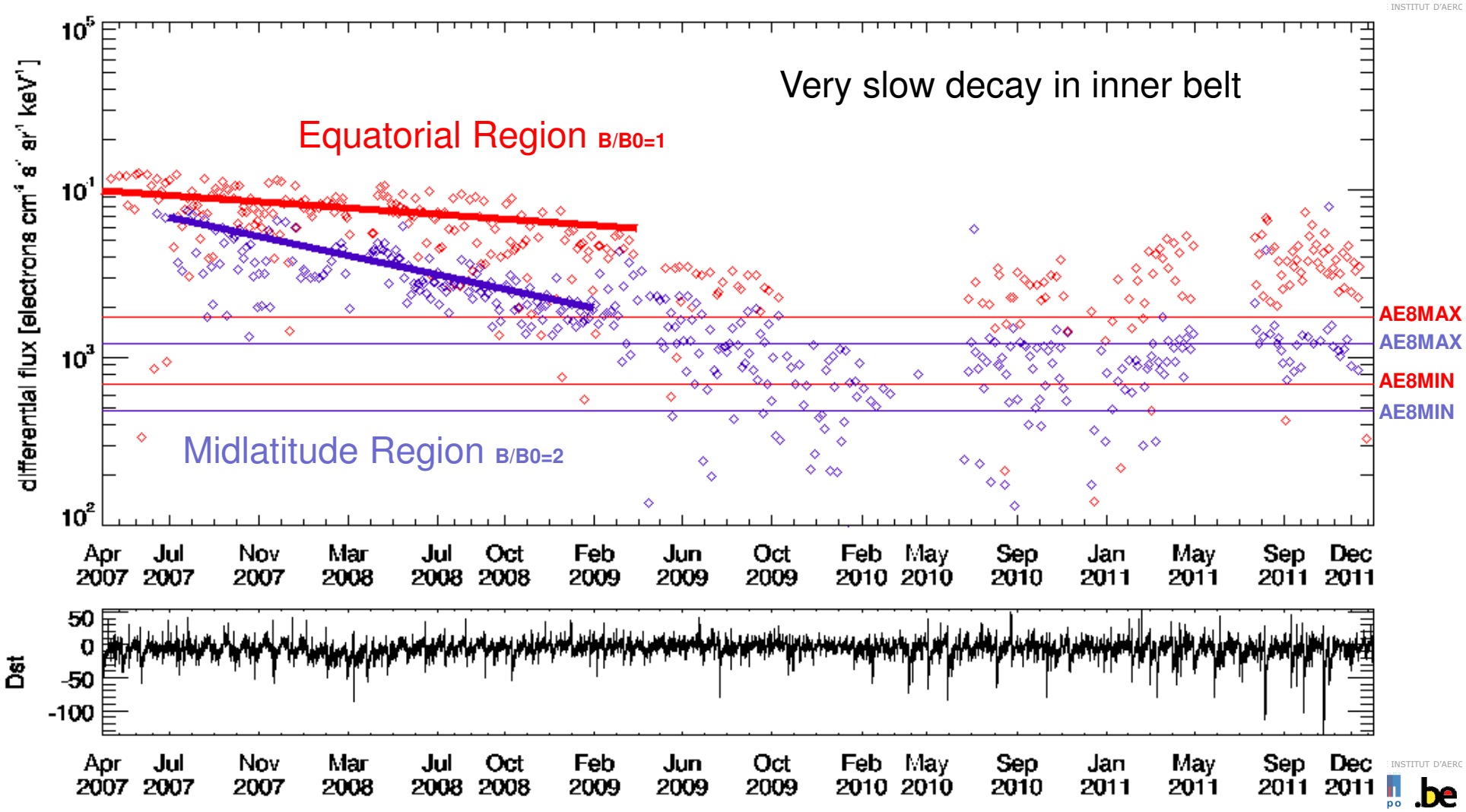

The Cluster spacecrafts fly along polar orbits, with a period of approximately 57h, and an initial perigee of about 4 R_E. Since 2007, the perigee of the Cluster orbit has moved closer to the Earth, down to about 1.3 R_E in the year 2010. The orbit has also changed from originally being polar to a much lower inclination.

Cluster satellites space coverage

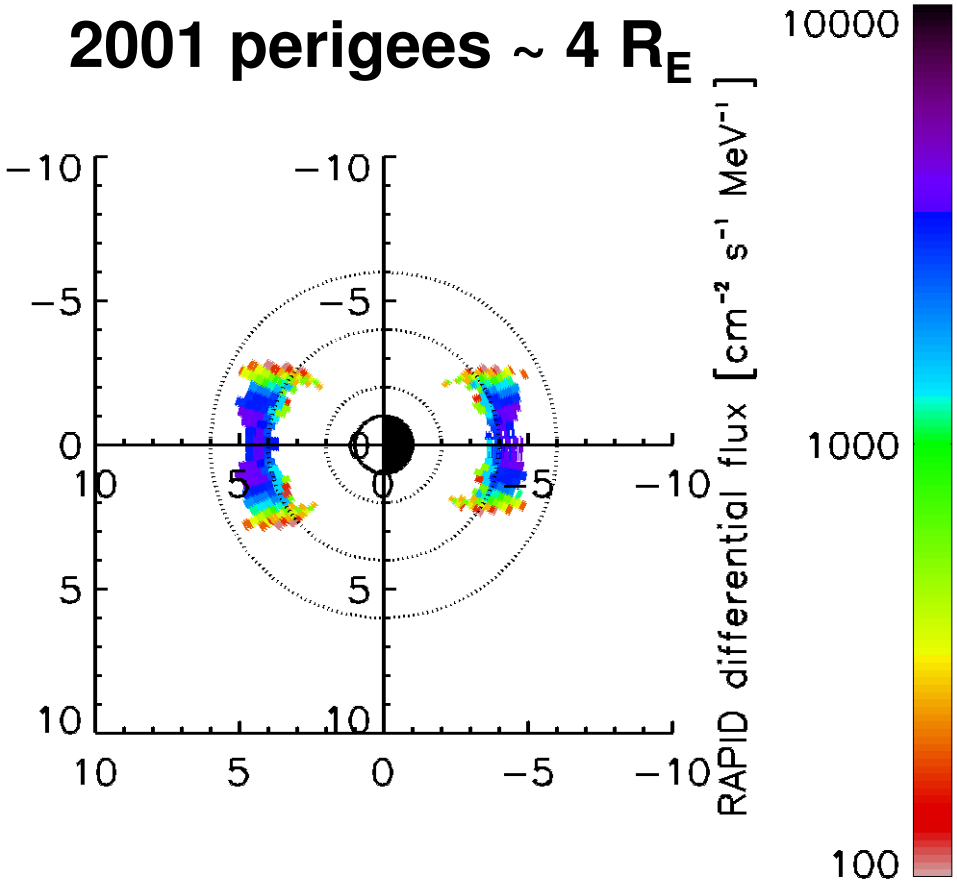

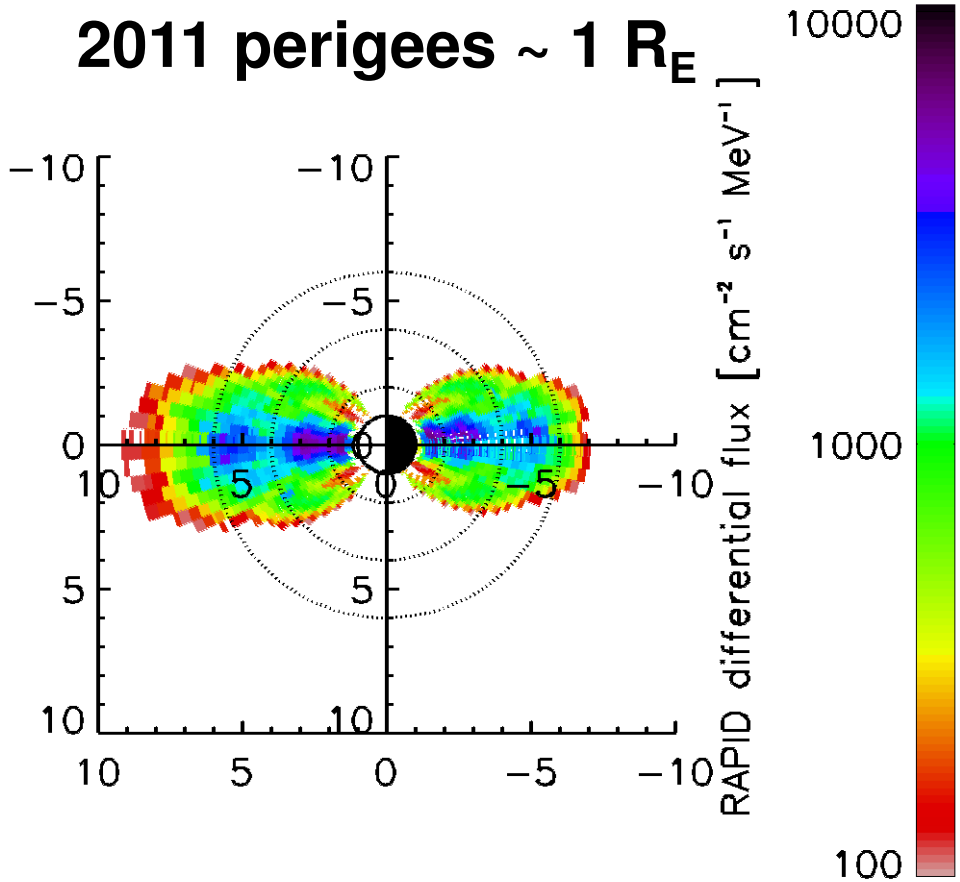

1 year averages are shown.

We have studied the dynamics of the radiation belts by analyzing the observations of the Cluster satellites. The outer electron belt can respond with 2 orders of magnitude to a geomagnetic storm, which is observed on the surface of the Earth by measuring the Dst index. The main phase of a geomagnetic storm is fast decrease of the Dst index. The Dst index is also related to the ring current.

L=5

40 - 50 keV

244 - 406 keV

Outer Electron Radiation Belt **is dynamic**

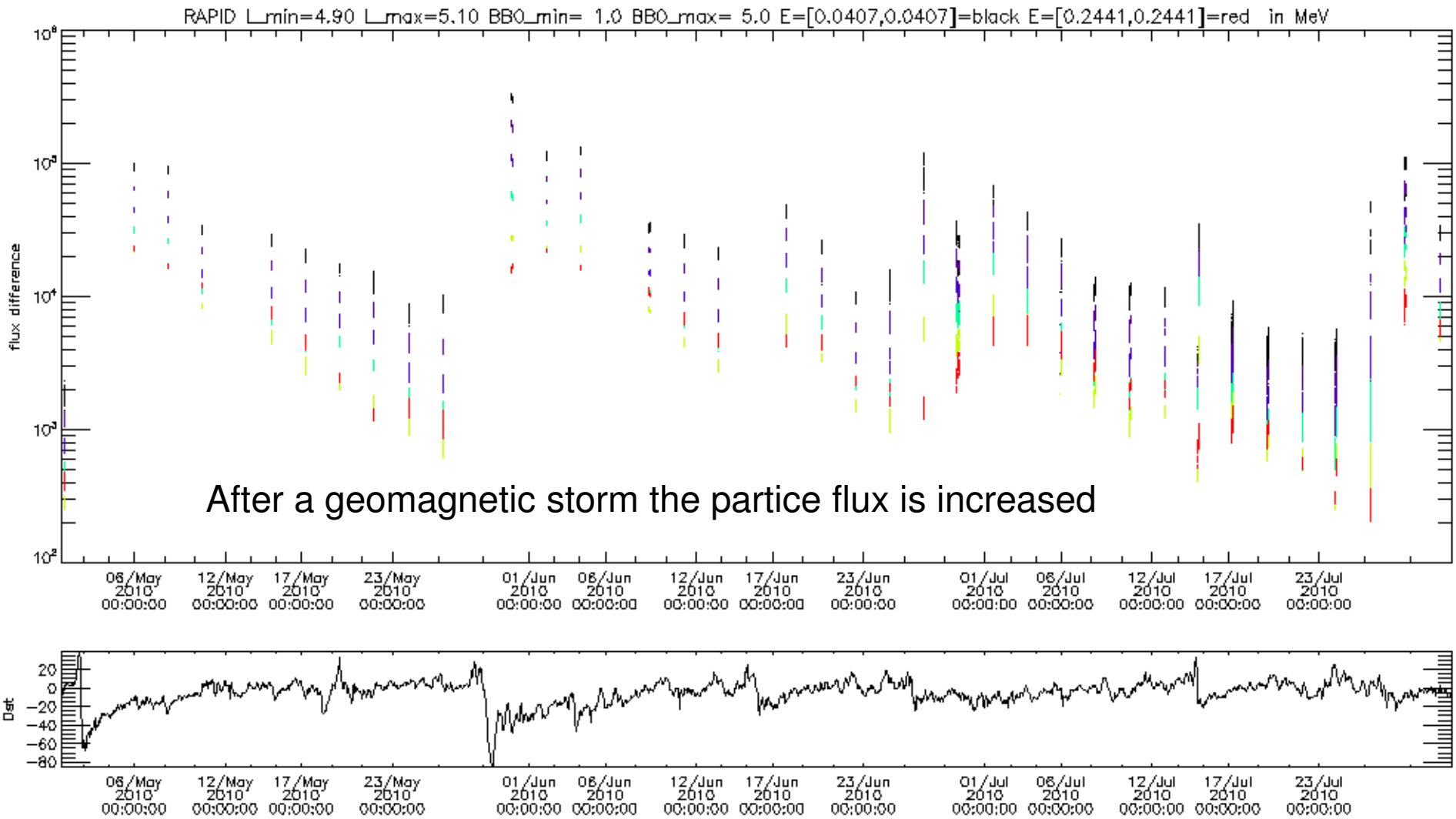

After a geomagnetic storm the partice flux is increased

The outer electron belt is most dynamic between 4 and 4.5 Earth radii, in all magnetic longitudes and for energies from 40 to 400 keV.

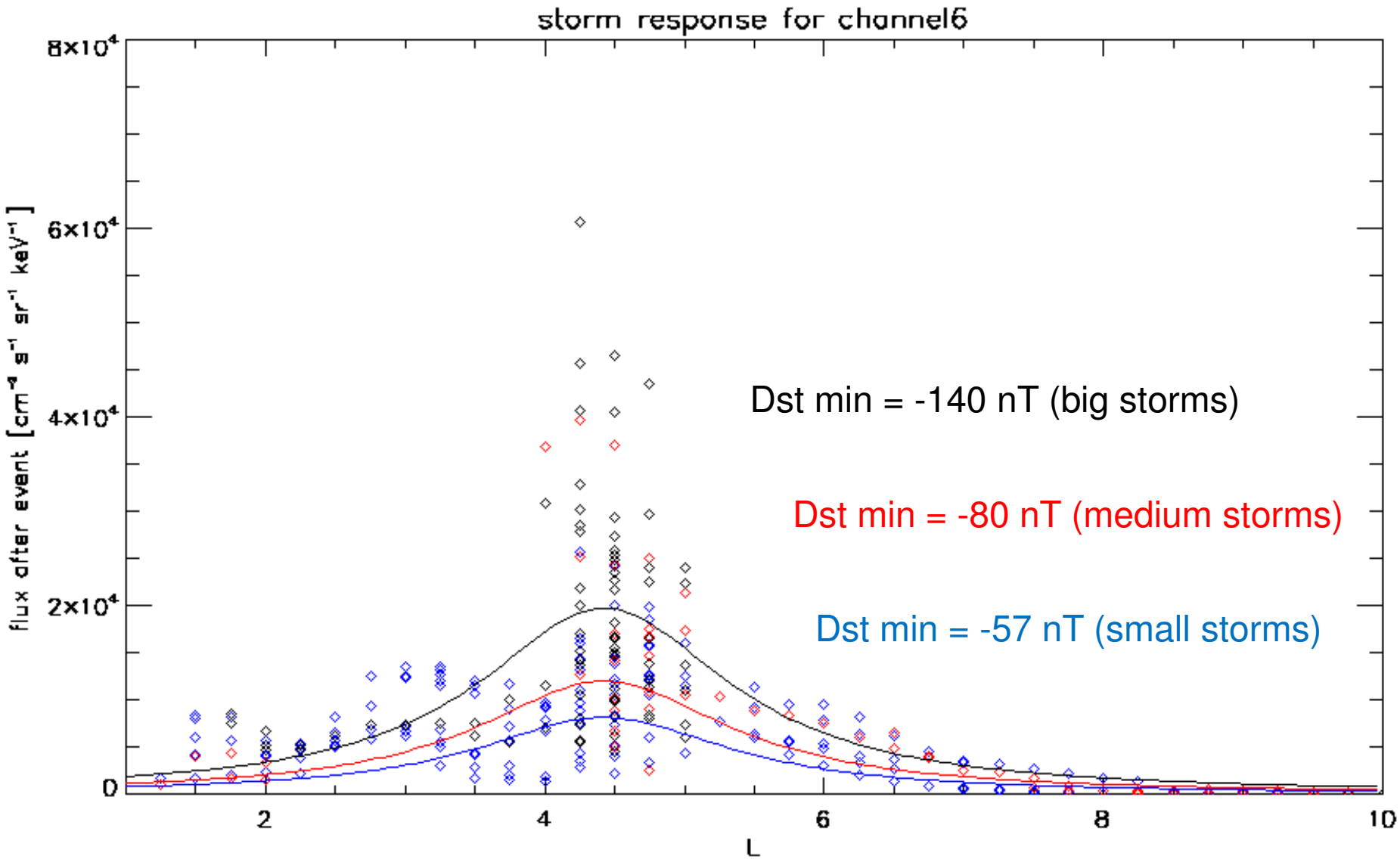

244 - 406 keV

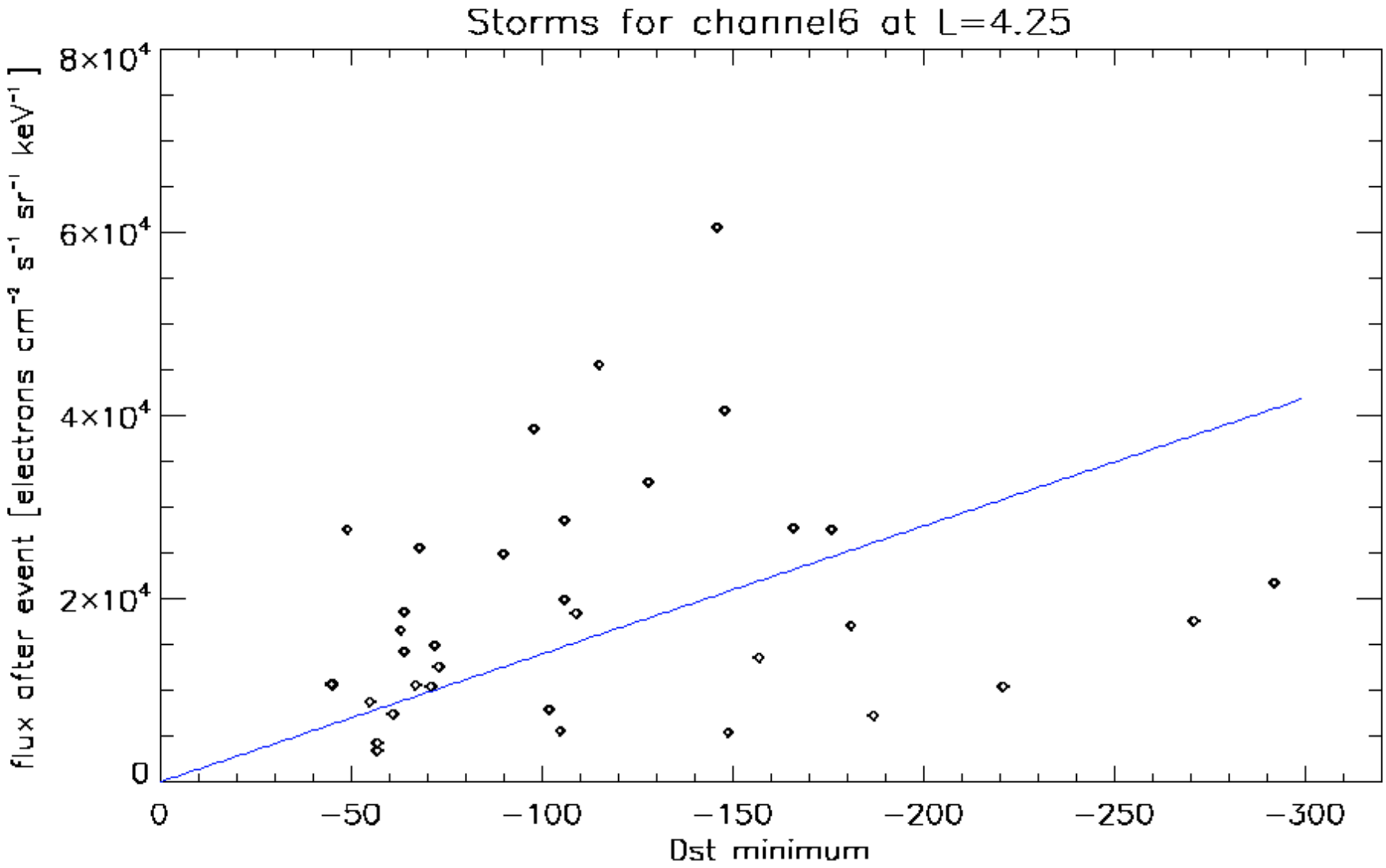
Storms for channel6 at L=4.25
flux after event [electrons cm^{-2} s^{-1} sr^{-1} keV^{-1}]
8×10^4
6×10^4
4×10^4
2×10^4
0
0
−50
−100
−150
−200
−250
−300
Dst minimum

40 - 50 keV

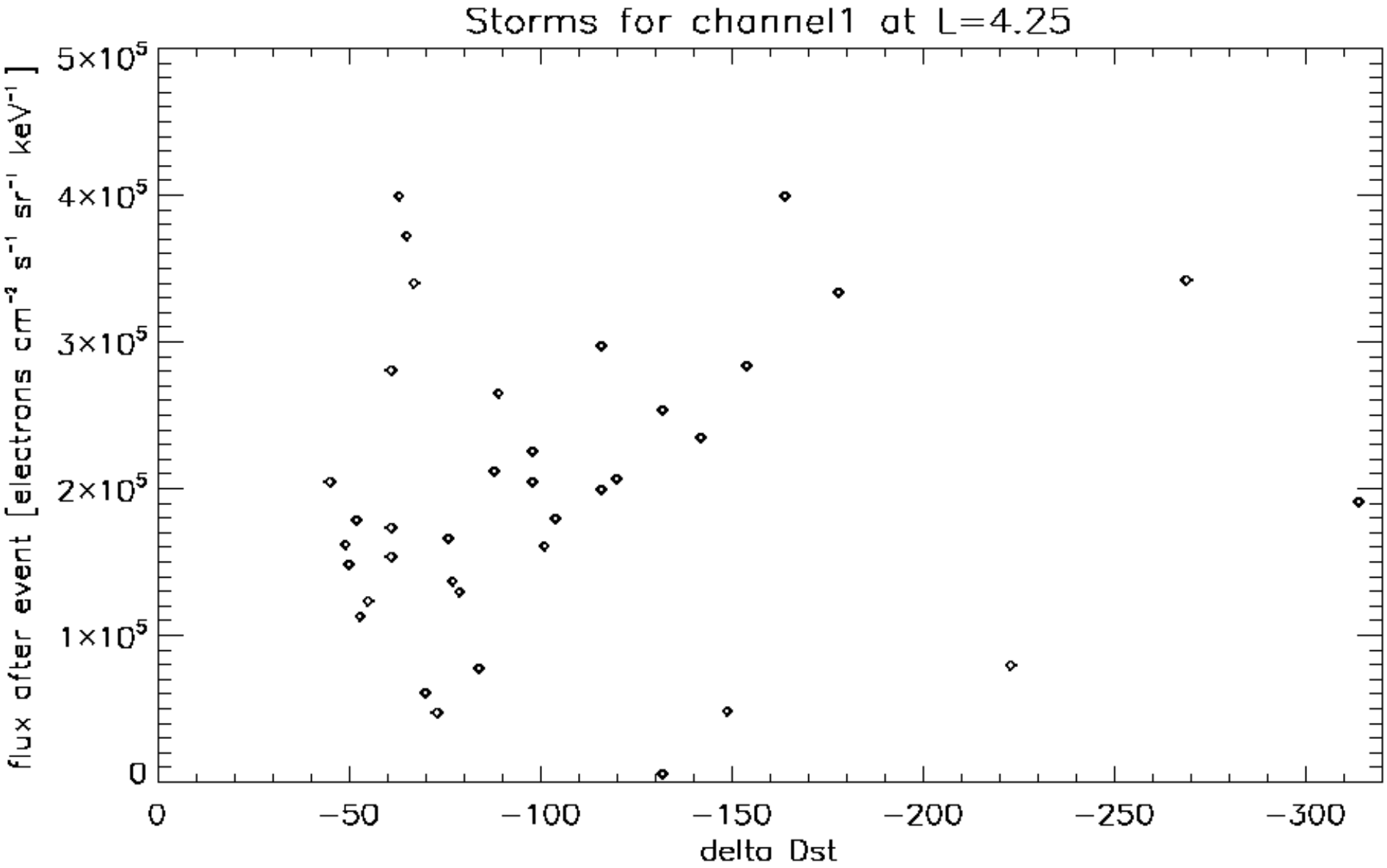
Storms for channel1 at L=4.25
flux after event [electrons cm⁻² s⁻¹ sr⁻¹ keV⁻¹]
5×10⁵
4×10⁵
3×10⁵
2×10⁵
1×10⁵
0
0
−50
−100
−150
−200
−250
−300
delta Dst

BIRA·IASB
aeronomie·be

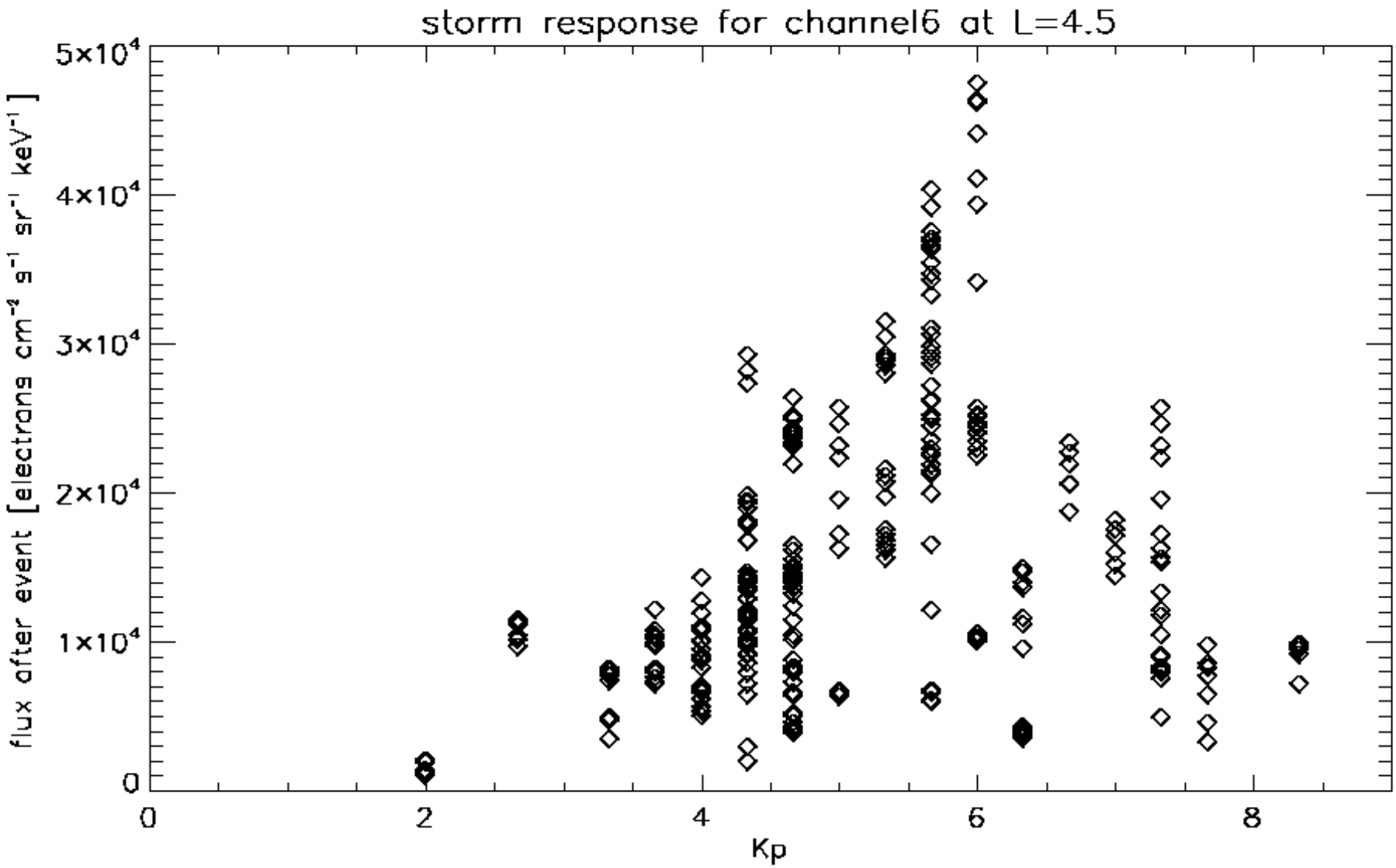

Relation between the geomagnetic indices Dst and Kp for the analyzed storms (with data for L=4.5).

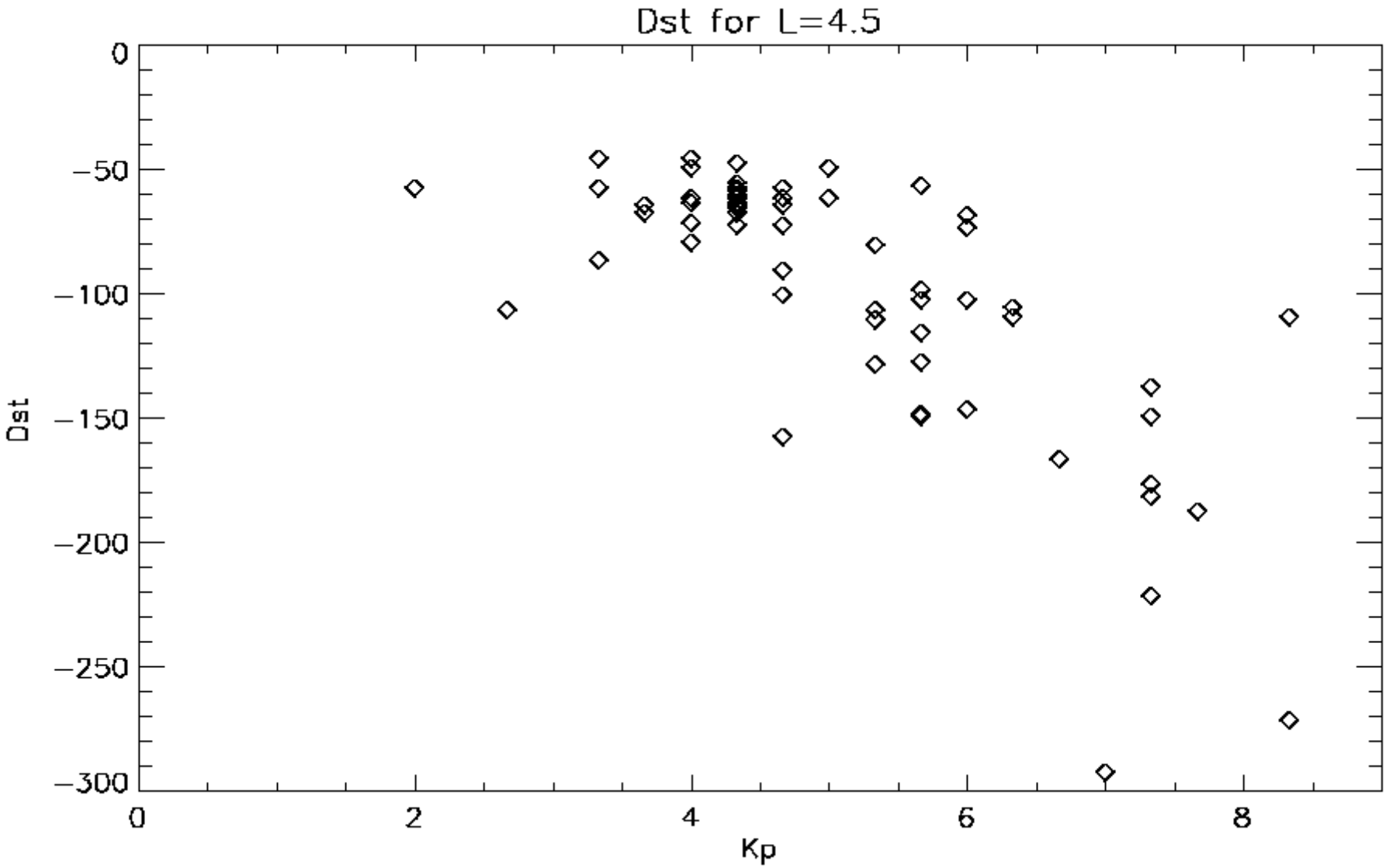

Our radiation belt model in the meridian plane for electrons with an energy of 300 keV.

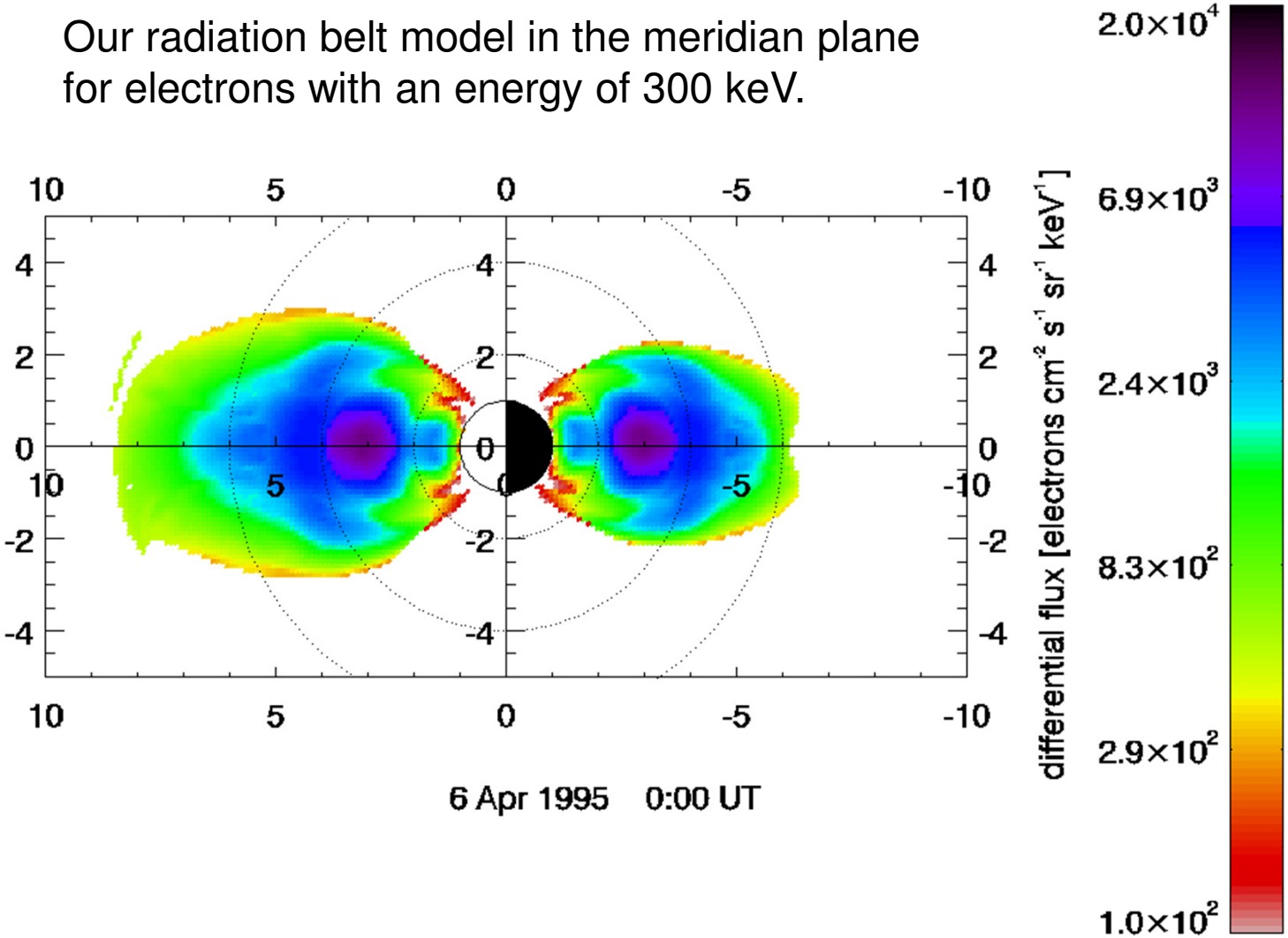

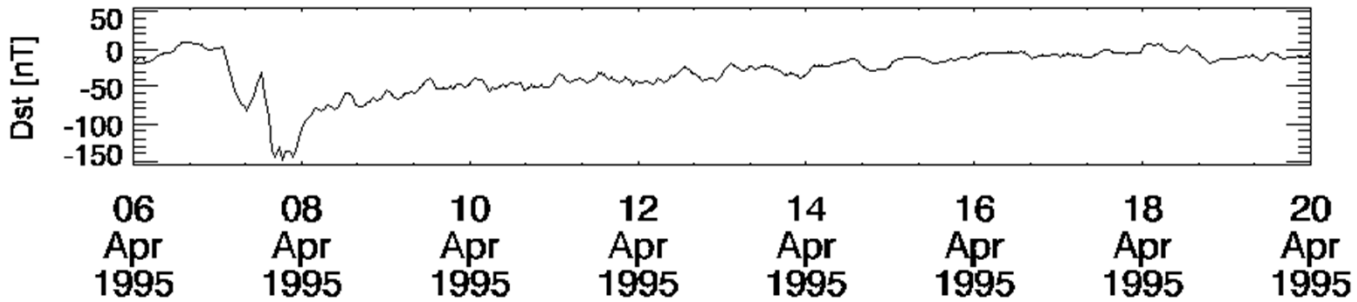

LETTERS
PUBLISHED ONLINE: 29 JANUARY 2012 | DOI: 10.1038/NPHYS2185
nature physics

Explaining sudden losses of outer radiation belt electrons during geomagnetic storms

Drew L. Turner[1,2]★, Yuri Shprits[1,2,3], Michael Hartinger[1] and Vassilis Angelopoulos[1,2]

Figure 1 | Overview of solar wind, geomagnetic indices, electron flux and ULF wave activity during the 06 January 2011 storm and dropout event. a, Solar wind dynamic pressure P_{Dyn} and speed from the OMNI dataset. **b**, Interplanetary magnetic field (IMF) total field strength B_{Tot} and Z-component in Geocentric Solar Magnetospheric coordinates B_Z. These exhibit the clear features of the CIR, with the initial compressed slow solar wind, the compressed fast wind segment associated with a strong southward IMF component, and the fast solar wind stream following behind them. The period of negative B_Z results in enhanced substorm activity. **c**, The Dst and Kp indices, both calculated using arrays of ground magnetometers. Dst shows a small storm, which is typical for CIRs, with a minimum value of greater than −50 nT, while Kp of 5.7 during the storm's main phase implies very active geomagnetic conditions. **d**, GOES-13 > 800 keV electron fluxes (#$cm^{-2}s^{-1}sr^{-1}$) measured from geosynchronous orbit showing the main phase flux dropout and subsequent recovery phase enhancement. **e**, McGrath ground station (MCGR) magnetometer data, D-component (∼east), with the d.c. field removed (No-d.c.). Enhanced ULF wave activity is evident during the entirety of the storm. The blue shaded periods marked by dashed lines indicate the overlap with the periods shown in **f** and **g**. **f**,**g**, The TH-A power spectral densities for the magnetic field magnitude (d.c. field removed) exhibiting ULF waves at frequencies comparable to outer belt electron drift frequencies. **f**, The TH-A inbound pass on 05–06 January during the quiet time before the storm. **g**, The following inbound pass during the main phase and flux dropout.

What happens during a geomagnetic storm?

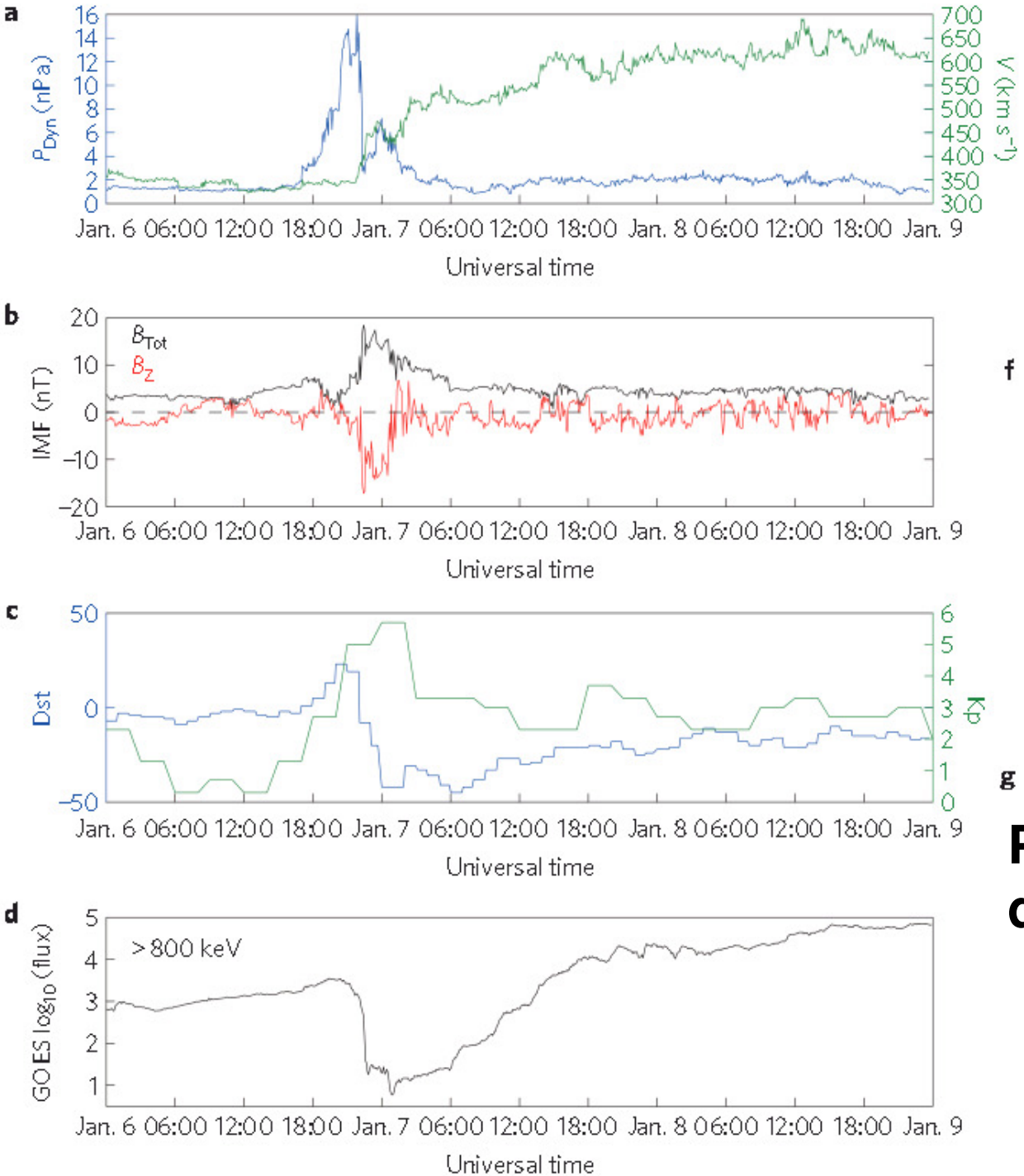

Outer belt
L ~ 5 R_E
6 January 2011

f

The decrease of the Dst index is the main phase of the geomagnetic storm.

g

Particle flux dropout during main phase!

Particle flux dropout during main phase!

We searched in the Cluster data for measurements during a main phase of a geomagnetic storm.

Events found: 31 March 2001, 21 October 2001, 26 September 2011, 19 May 2002, 11 October 2010, …
not enough data to make statistic.

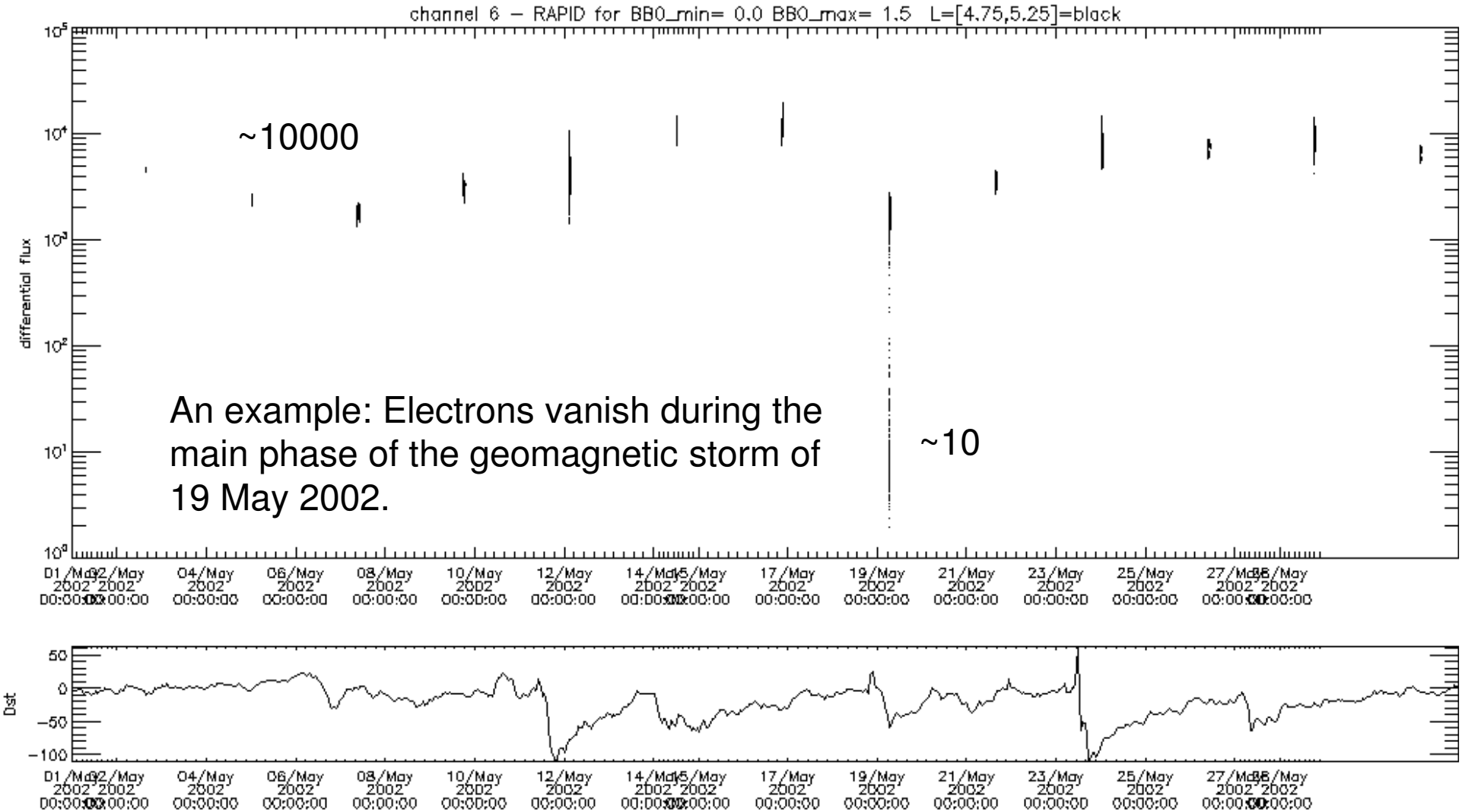

We launch a proton at L=4 in the equatorial plane with an energy of 1MeV and simulate a geomagnetic storm.

Relativistic Test Particle Simulation

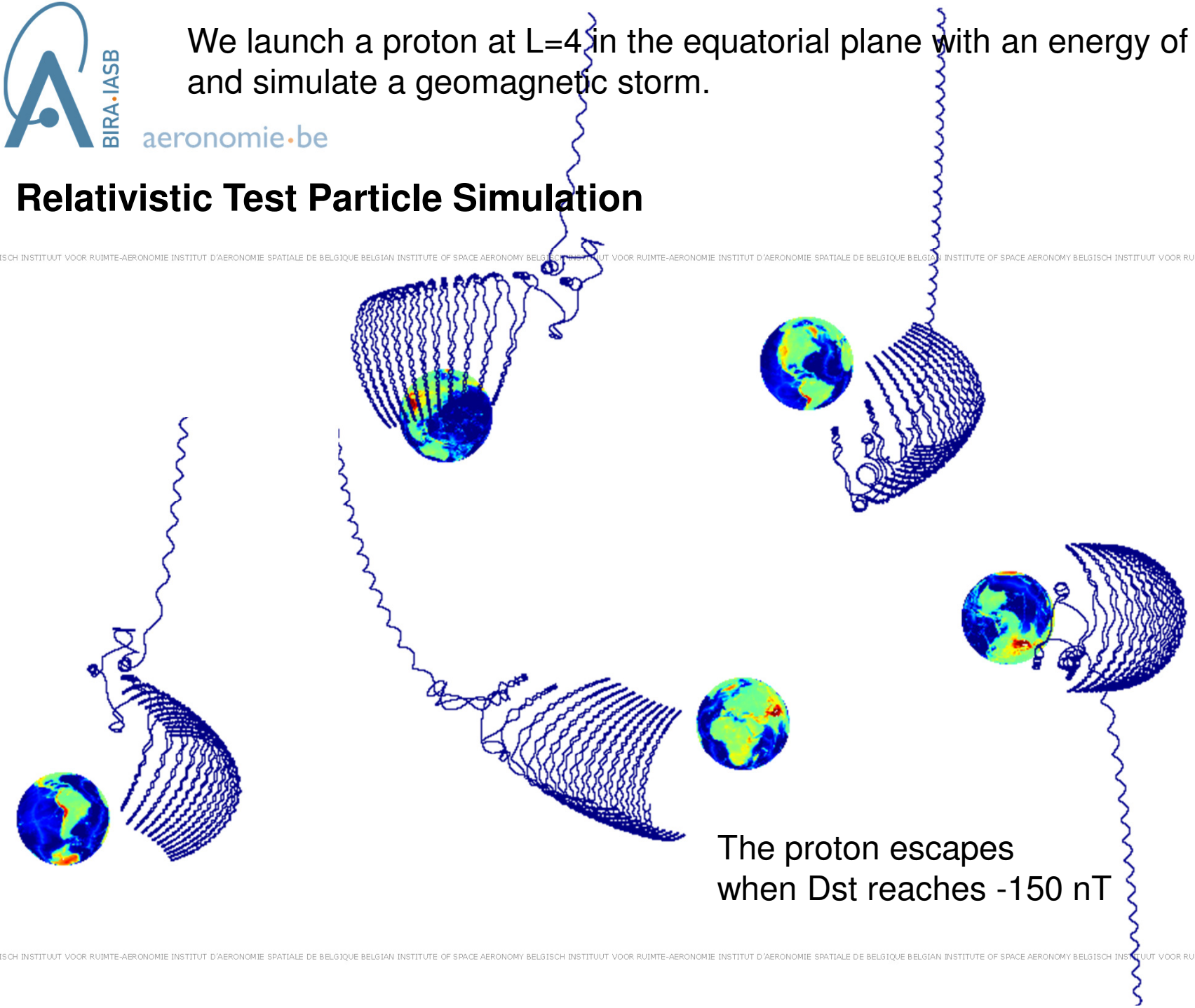

The proton escapes when Dst reaches -150 nT

Main phase of geomagnetic storm:
Magnetic field decreases to -200 nT

1MeV Proton

Proton decelerates

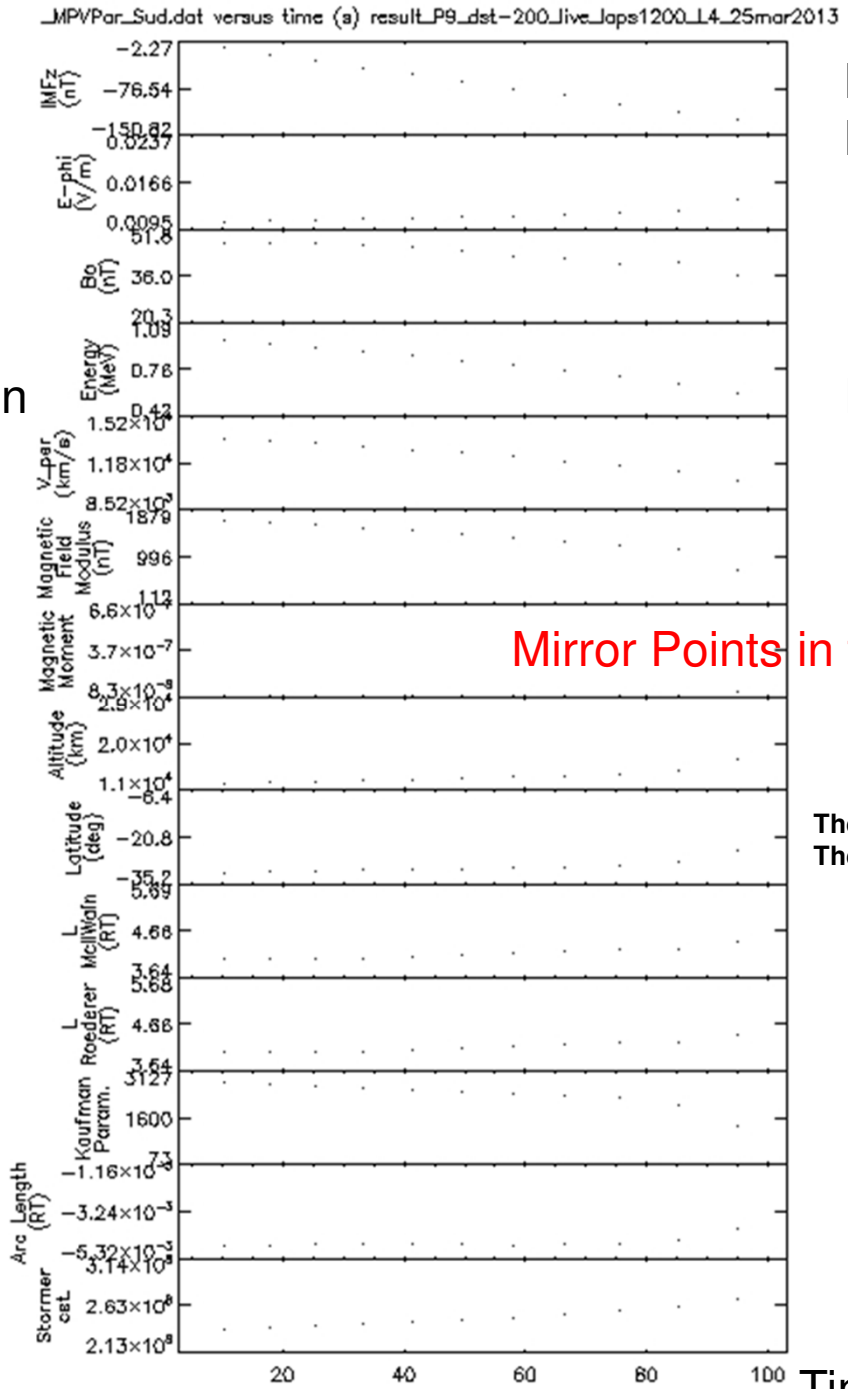

Mirror Points in the Southern hemisphere

The equatorial pitch angle at launch is 30 degrees.
The latitude of the mirror points only depends on the pitch angle.

L=4

Proton escapes
when Dst reaches -150 nT

Time in seconds

Comparisons simulations and observations

Particle dropouts and L shell diffusion (radial diffusion) by Betatron effect

We compare the results of the simulations with the observations of the Cluster satellites,
which show a particle dropout during the main phase of a geomagnetic storm in the outer belt and no response in the inner belt.

An electron with an energy of 300 keV corresponds with the energy channel 6
of the RAPID instument on Cluster.

According to the observed pitch angle distribution, most electrons stay equatorially.
So, we simulate here an electron with a pitch angle of 85 degrees.

We launch a test particle at 3 Earth radii and at 6 Earth radii to compare with the inner and outer belt.

Effects of concomitancy of adiabatic Betatron deceleration & acceleration (i),
of up & down lifting of mirror points altitudes (ii),
and of pitch angle scattering (iii) during geomagnetic storms

J.F. Lemaire K. Borremans V. Pierrard
Belgian Institute for Space Aeronomy – Brussels

EGU General Assembly 2013, Session ST2.3: EGU2013-13889

Electron with
Cluster energy channel 6
escapes at L=6
when Dst becomes < -50 nT

300 keV
Electron
at L=6

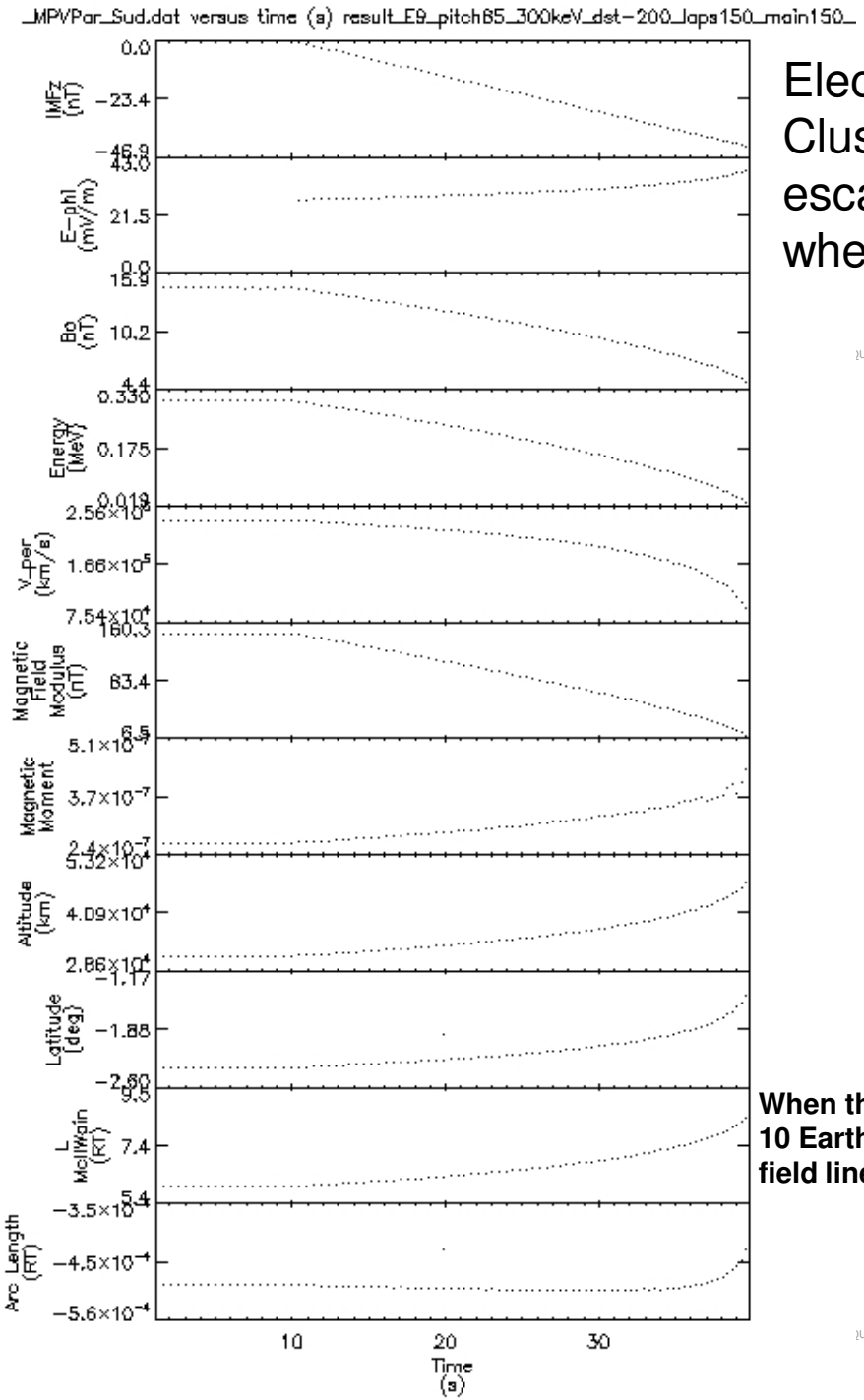

Dynamic Outer Belt

McIlwain L

When the L shell parameter becomes larger than 10 Earth radii, then you are on an open magnetic field line.

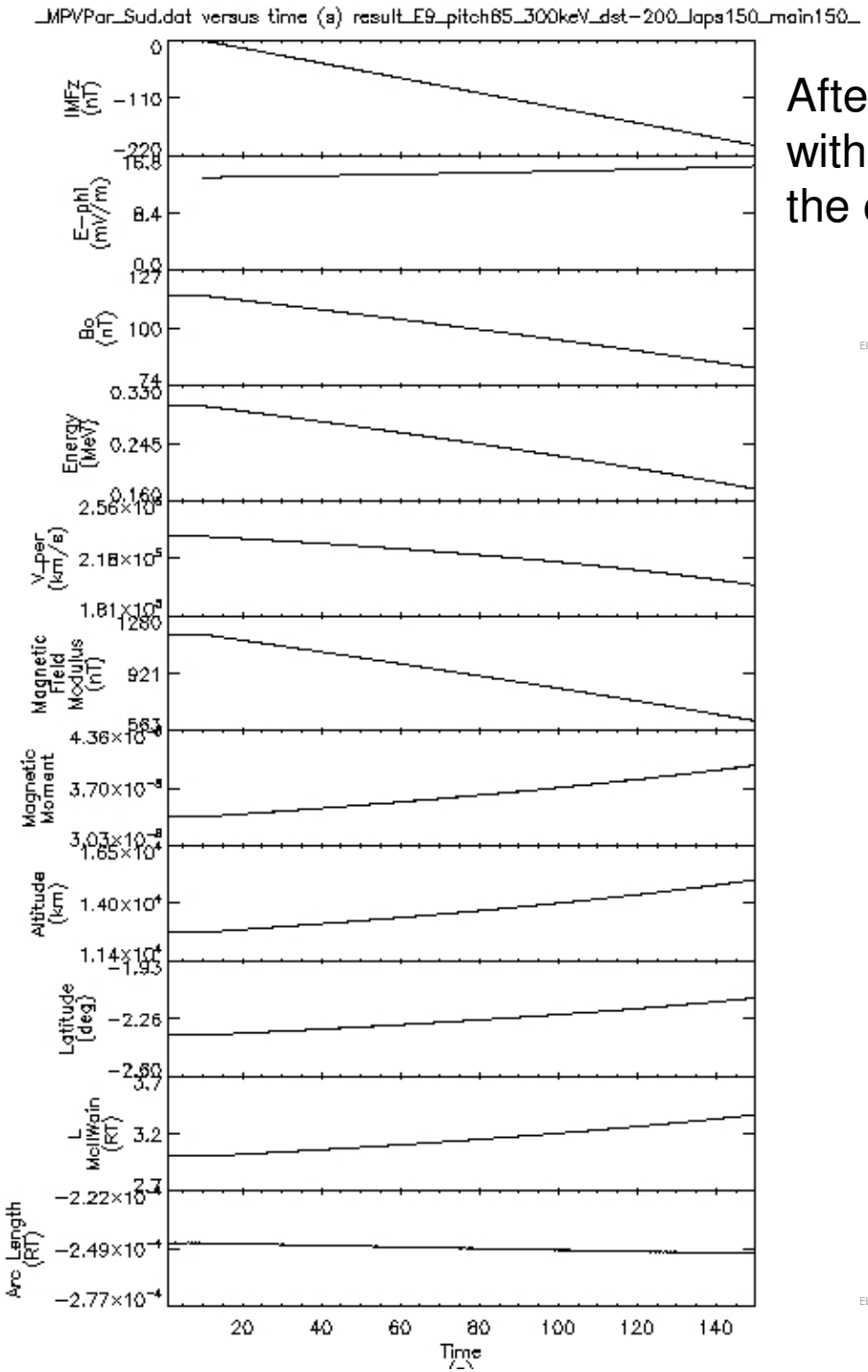

After a geomagnetic storm with a main phase going to -200nT the electron is still trapped.

300 keV Electron at L=3

Stable Inner Belt

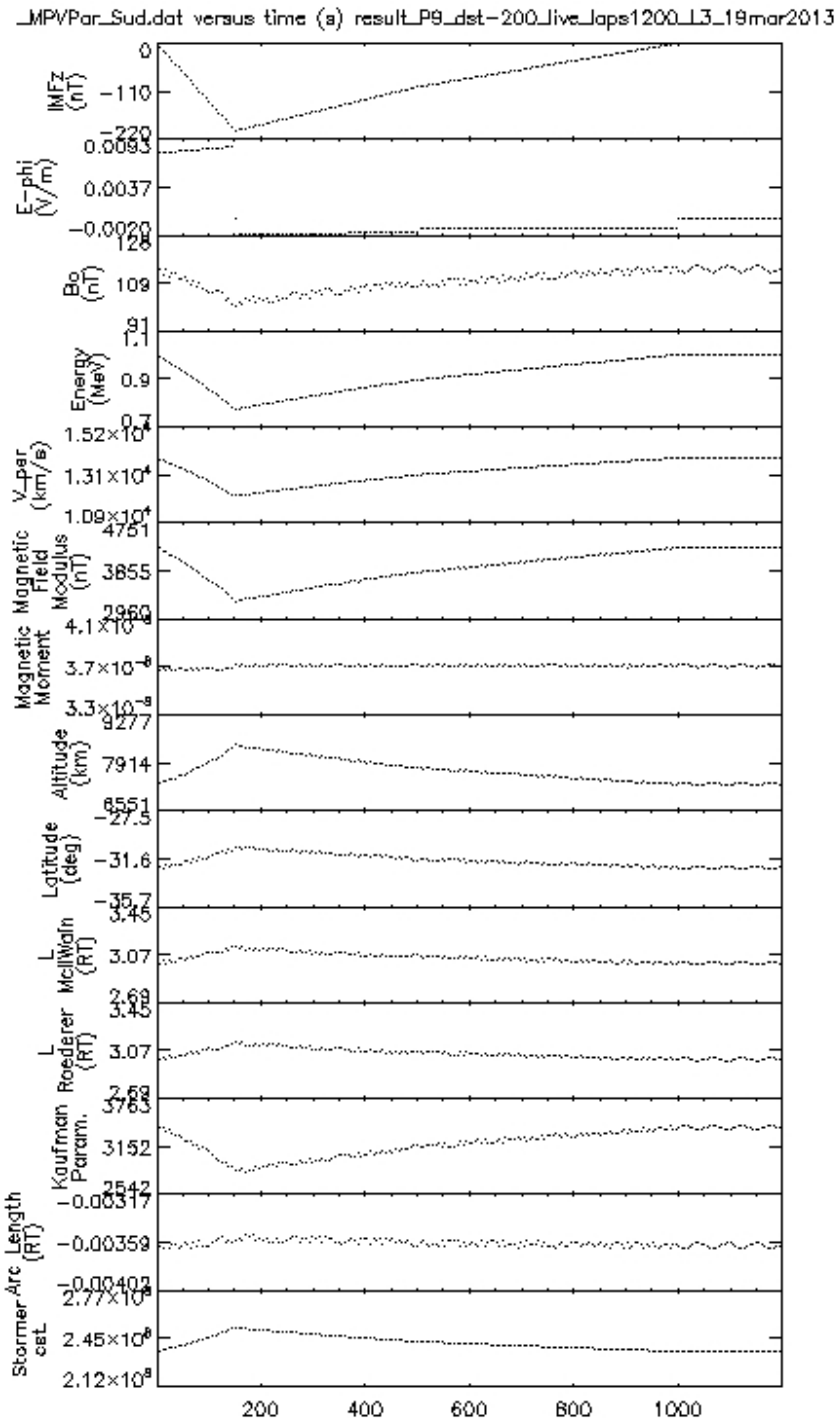

Main phase + recovery phase

Proton of 1 MeV at L=3 remains trapped.

Deceleration during main phase.
Acceleration during recovery phase.
After the storm the energy of the proton is still 1 MeV.

Altitude of mirror points determines if a particle collides with the atmosphere or not.

During the main phase the mirror points are uplifted and the particle drifts radially outward.

During the recovery phase the mirror points fall back and the particle drifts radially inward.

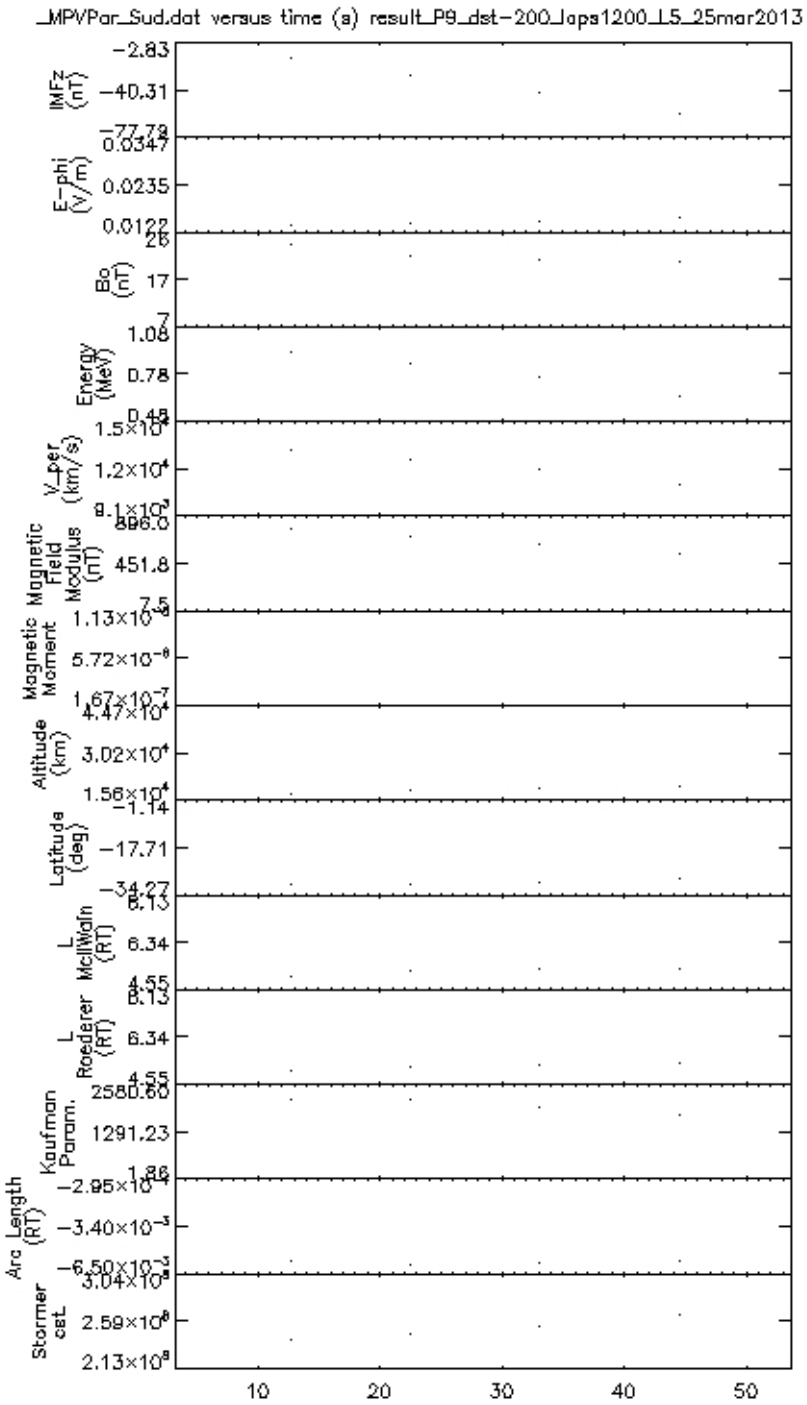

Proton of 1 MeV at L=5 escapes when Dst reaches -80 nT.

For larger L shells, the particle escapes even faster.

TE-AERONOMIE INSTITUT D'AERONOMIE SPATIALE DE BELGIQUE BELGIAN INSTITUTE OF SPACE AERONOMY BELGISCH INSTITUUT VOOR RUIMTE-AERONOMIE INSTITUT D'AERO

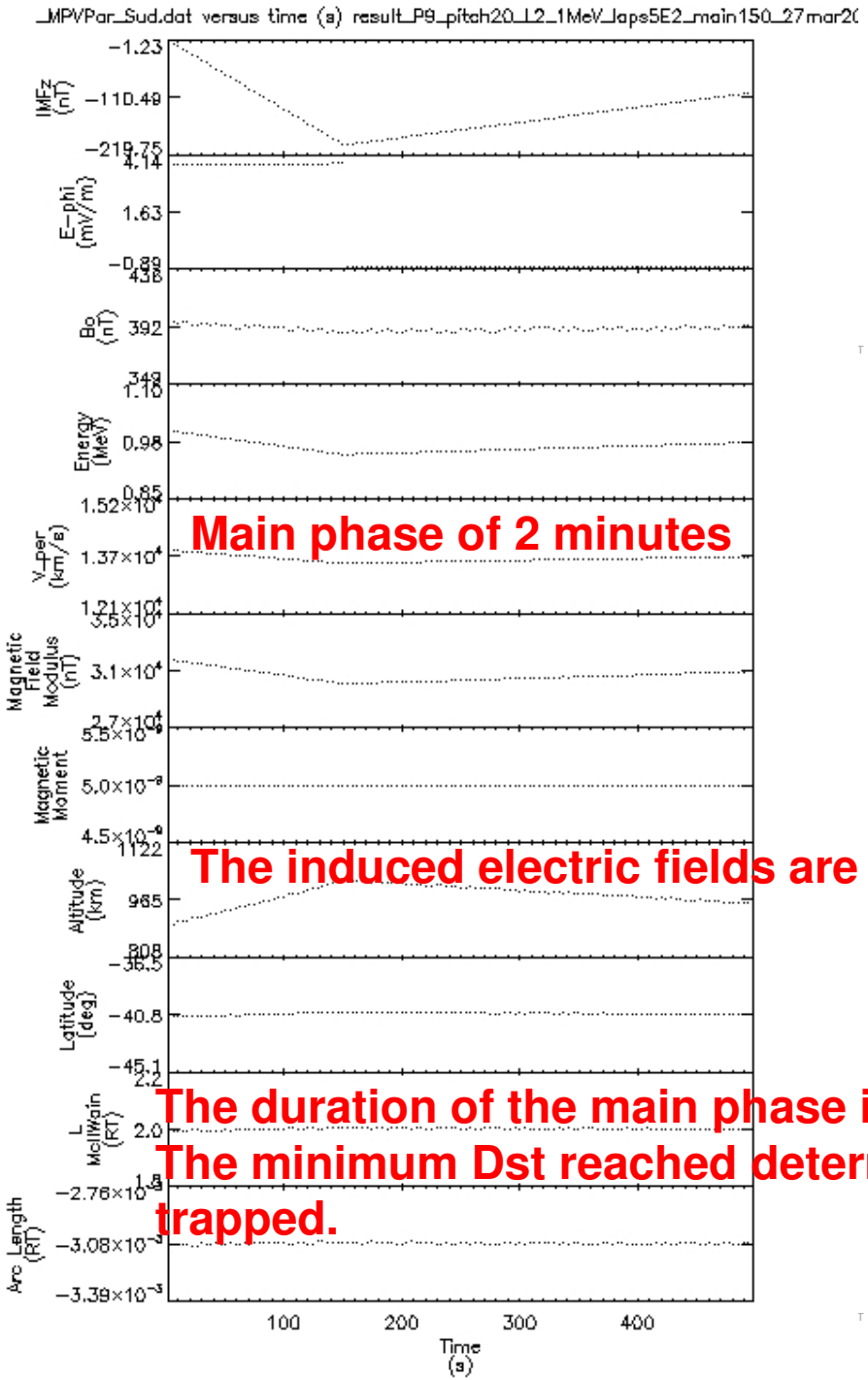

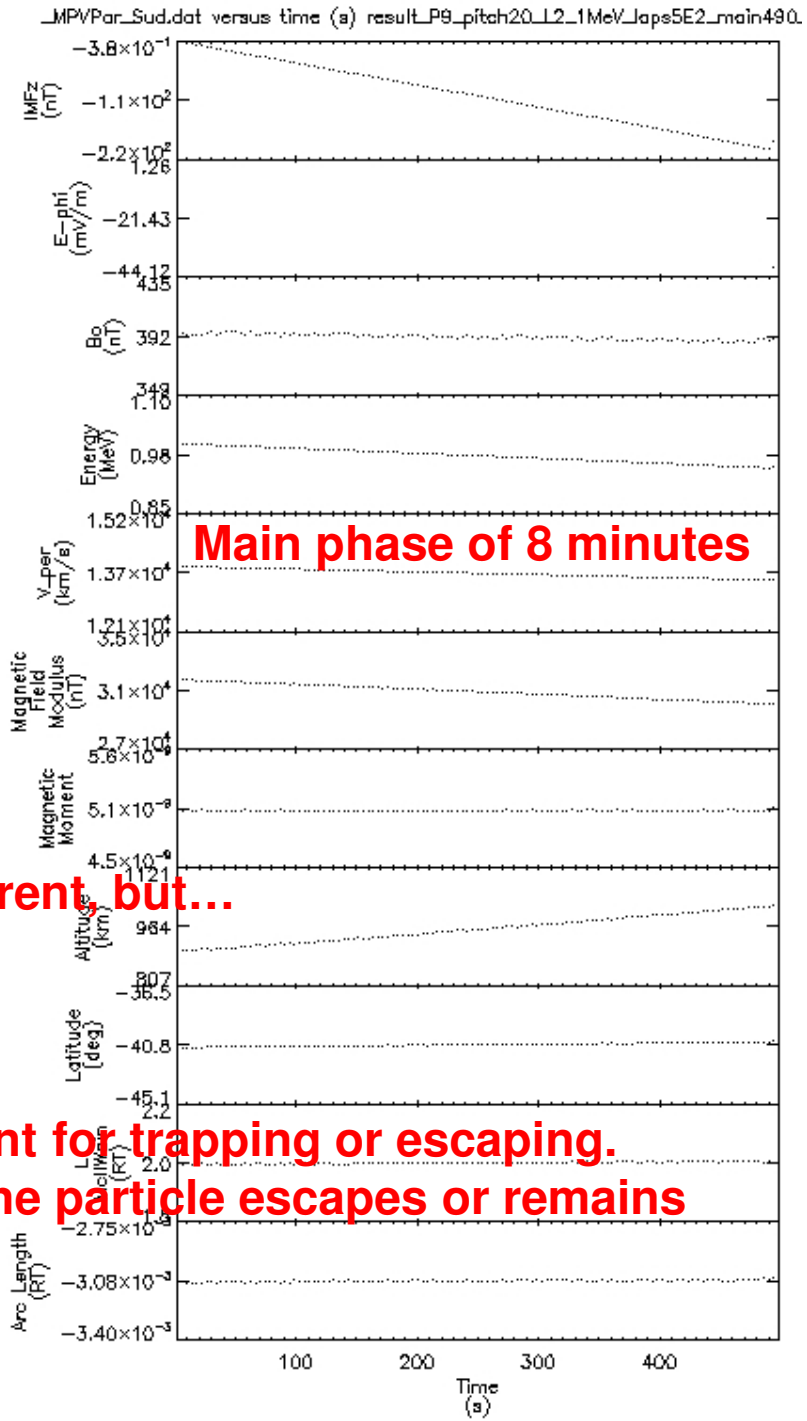

Main phase of 2 minutes

Main phase of 8 minutes

The induced electric fields are very different, but…

The duration of the main phase is irrelevant for trapping or escaping.
The minimum Dst reached determines if the particle escapes or remains trapped.

T VOOR RUIMTE-AERONOMIE INS

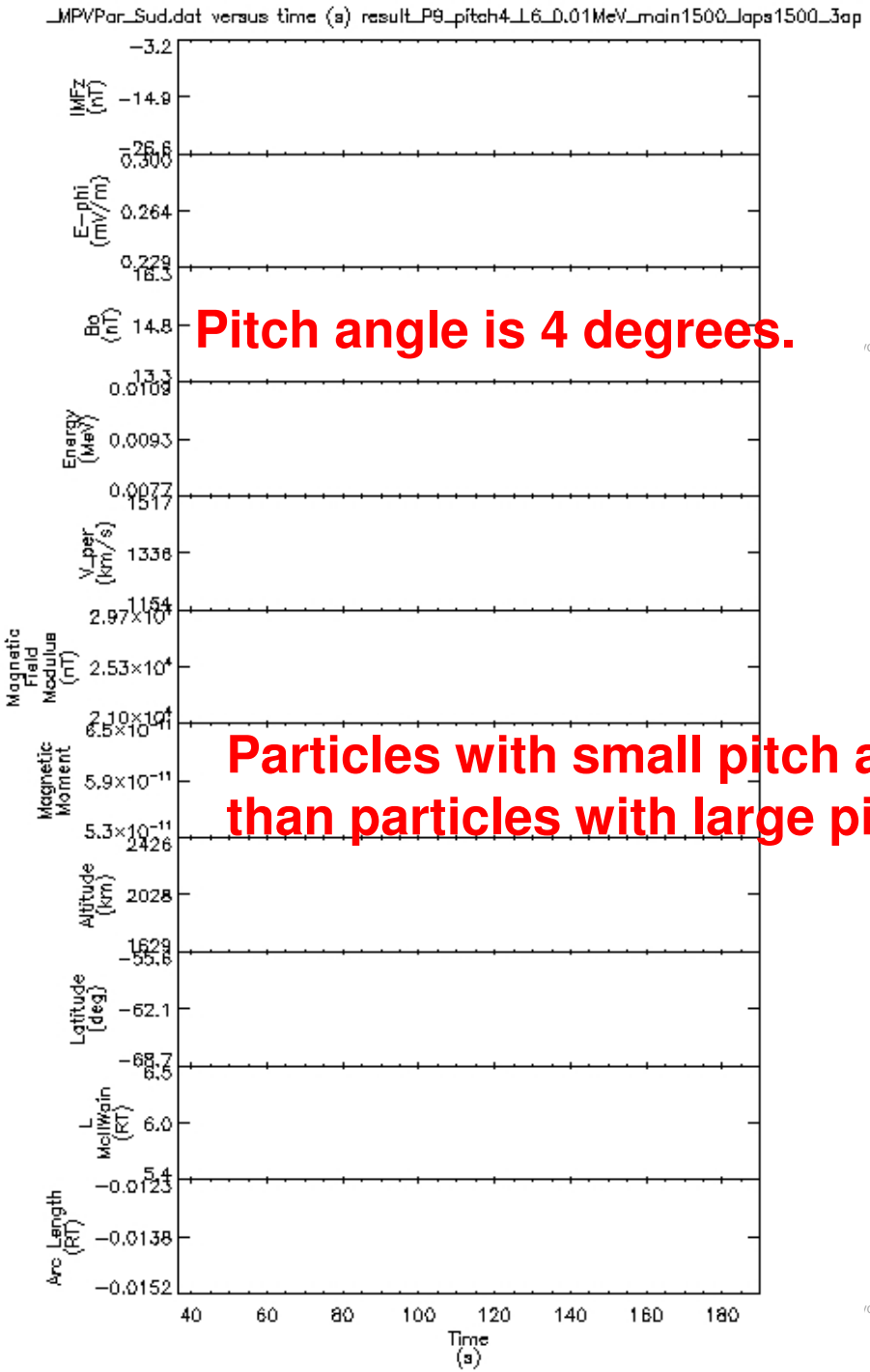

Pitch angle is 4 degrees.

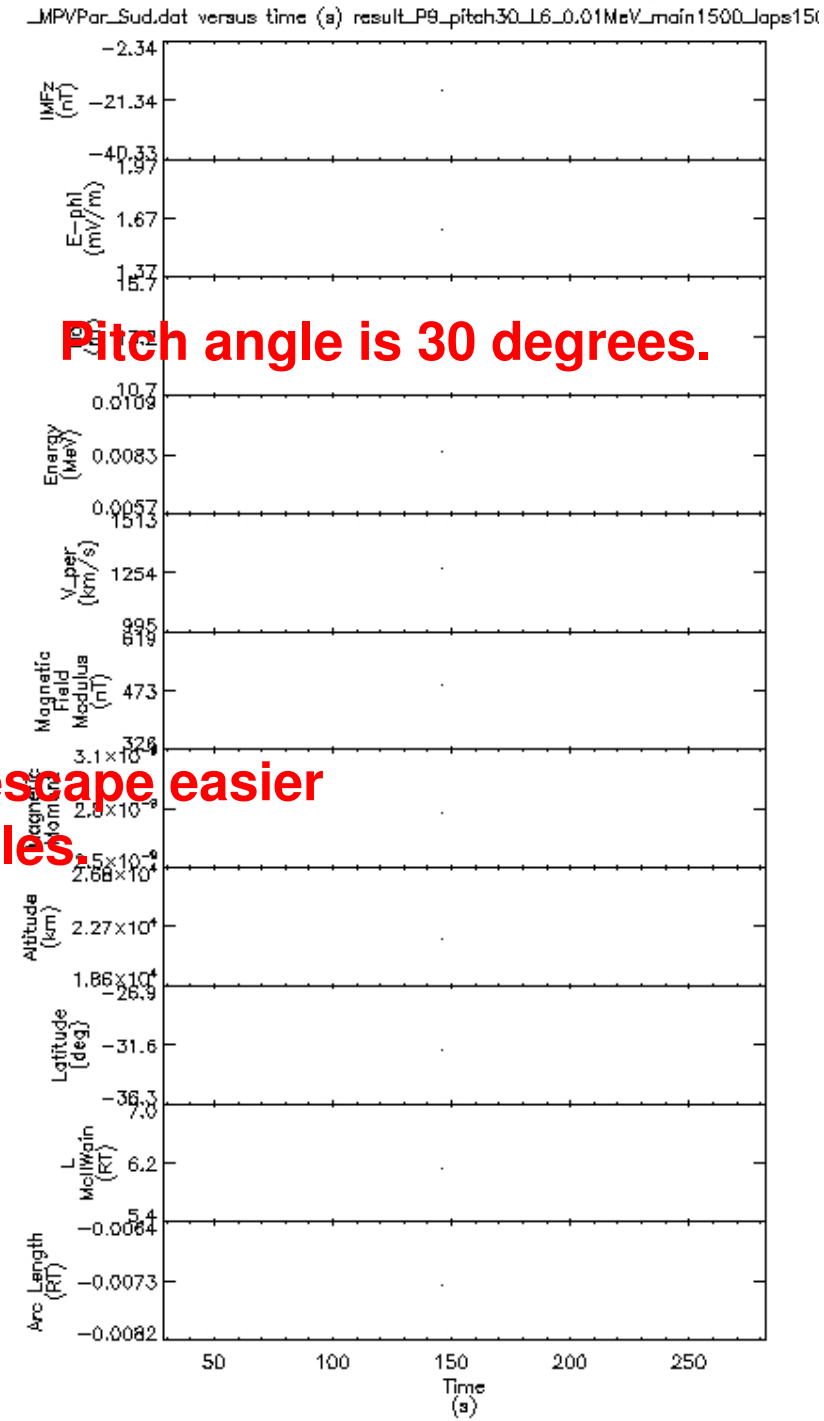

Pitch angle is 30 degrees.

Particles with small pitch angles escape easier than particles with large pitch angles.

South Atlantic Anomaly

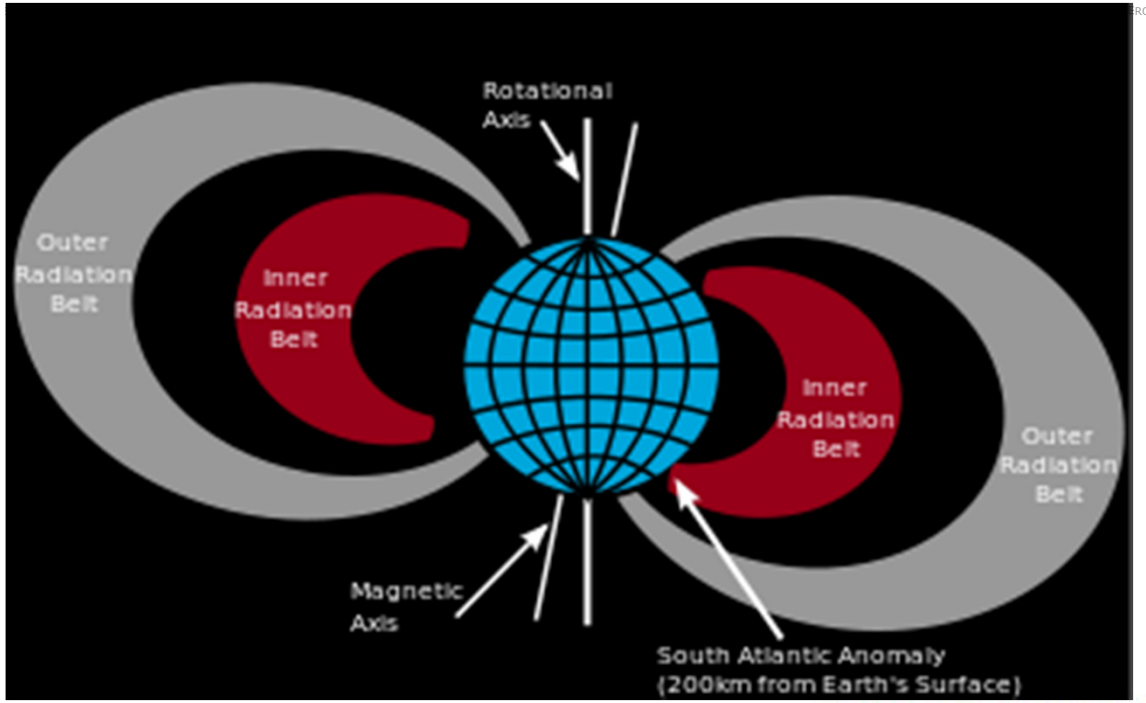

200 km from Earth's surface

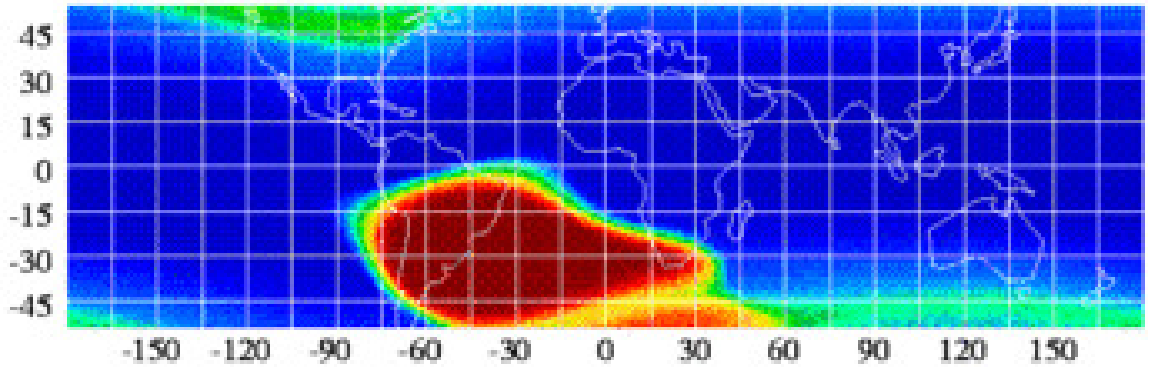

Space radiations

Spectra from EPT on Proba-V (launched on 7 May 2013)

e^-: 500 keV-10 MeV
p^+: 7 MeV-300 MeV
alpha: 27 MeV- 1 GeV

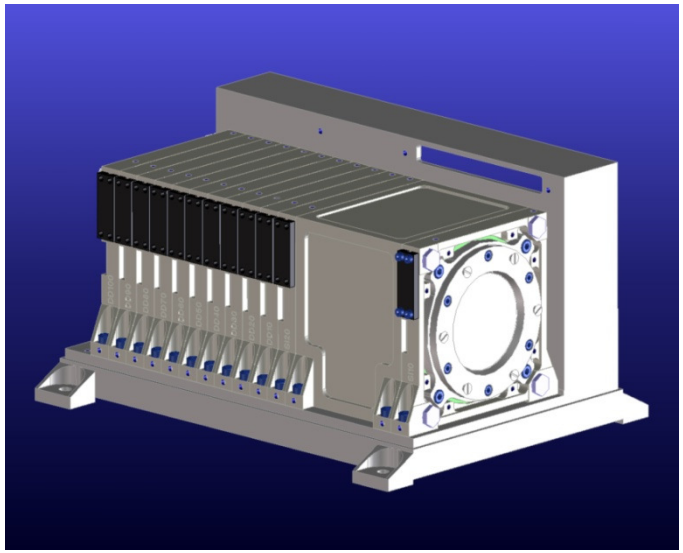

Dim:
130 x 160 x 210 mm^3

Mass:
4,6 kg

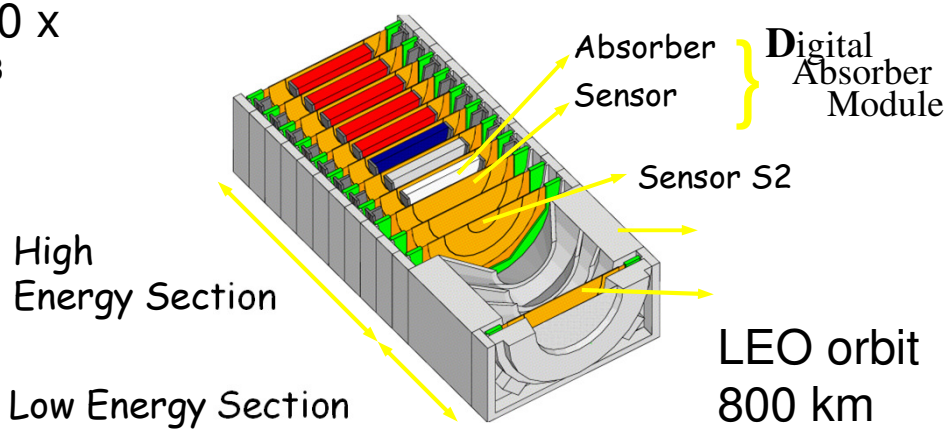

LEO orbit
800 km
98° inclin

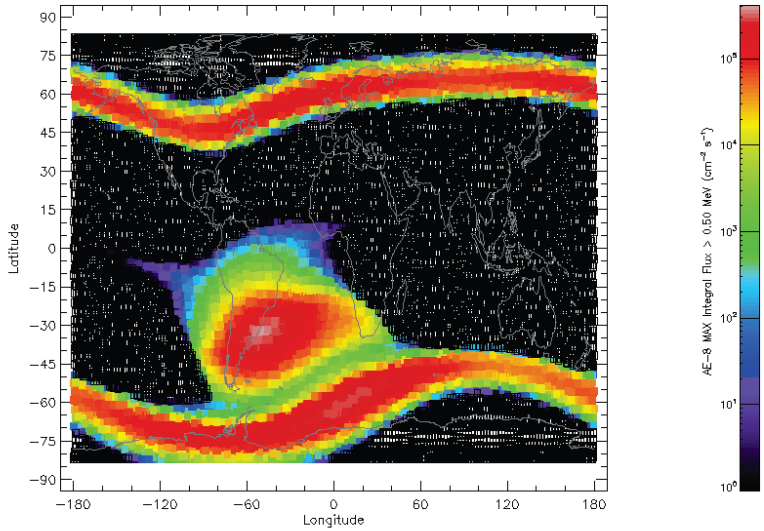

E>0.5 MeV electrons

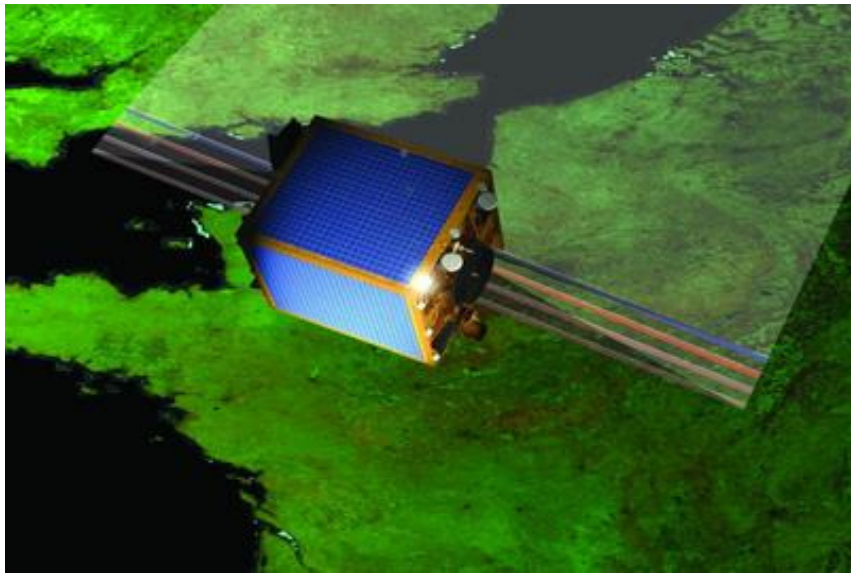

Conclusions

- **You can run the plasmasphere model on** http://www.spaceweather.eu
- **Observations of the RAPID instrument of the Cluster satellites are analyzed and a radiation belt model is being developed.**
- **After a geomagnetic storm the electron flux is increased in the outer belt.**
- **Then it exponentially decays away with a half life time of 3 days.**
- **In the inner belt there is no storm response. Inner electron belt is relatively stable.**
- **There is a slow decay with a half life time of several months.**
- **The decay is faster in the higher latitudes than in the equatorial plane.**
- **The inner belt was during 2007-2011 denser than AE8MIN and AE8MAX.**
- **In the outer electron belt the maximum particle flux is located at 4.25 Earth radii.**
- **The particle storm response is compared with the geomagnetic indices Dst and Kp.**
- **During the main phase of a geomagnetic storm there is a particle dropout, which is caused by the betatron effect.**
- **Outer belt electrons during a test particle simulation of a geomagnetic storm escape.**
- **Inner belt electrons remain trapped.**
- **The trapping or escaping is independent of the duration of the main phase.**
- **The minimum Dst reached determines if the particle escapes or remains trapped.**
- **High energy particles will escape easier than low energy particles.**
- **Particles with small pitch angles escape easier than particles with large pitch angles.**
- **During the main phase the particles will mirror at higher altitudes.**

Thank you!

Particle sensors aboard the twin Van Allen Probes revealed the existence of a transient, third radiation belt. Scientists observed the third belt for four weeks before a powerful interplanetary shock wave from the sun annihilated it. (28 Feb. 2013)